Physica Scripta

PAPER

Optimizing solar power generation forecasting in smart grids: a hybrid convolutional neural network -autoencoder long short-term memory approach

RECEIVED
17 May 2024

REVISED
26 July 2024

ACCEPTED FOR PUBLICATION
7 August 2024

PUBLISHED
22 August 2024

Ahsan Zafar[1,*], **Yanbo Che**[1,*], **Moeed Sehnan**[2], **Usama Afzal**[3], **Abeer D Algarni**[4] **and Hela Elmannai**[4]

[1] Key Laboratory of Smart Grid of Ministry of Education, School of Electrical and Information Engineering, Tianjin University, Tianjin 300072, People's Republic of China
[2] School of Electrical and Information Engineering, Tianjin University, Tianjin 300072, People's Republic of China
[3] School of Microelectronics, Tianjin University, Tianjin 300072, People's Republic of China
[4] Department of Information Technology, College of Computer and Information Science, Princess Nourah bint Abdulrahman University, PO Box 84428, Riyadh 11671, Saudi Arabia
[*] Authors to whom any correspondence should be addressed.

E-mail: ahsanuetp@hotmail.com, ybche@tju.edu.cn, sehnan@tju.edu.cn, mohammadusamafzal7@gmail.com, adalqarni@pnu.edu.sa and hselmannai@pnu.edu.sa

Keywords: renewable energy, smart grids, time series forecasting, AELSTM, hybrid HCAELSTM model

Abstract

Incorporating zero-carbon emission sources of energy into the electric grid is essential to meet the growing energy needs in public and industrial sectors. Smart grids, with their cutting-edge sensing and communication technologies, provide an effective approach to integrating renewable energy resources and managing power systems efficiently. Improving solar energy efficiency remains a challenge within smart grid infrastructures. Nonetheless, recent progress in artificial intelligence (AI) techniques presents promising opportunities to improve energy production control and management. In this study, initially, we employed two different Machine learning (ML) models: Recurrent Neural Network (RNN) and Long Short Term Memory (LSTM), to forecast solar power plant parameters. The analysis revealed that the LSTM model performed better than RNN in terms of Mean Absolute Percentage Error (MAPE), Mean Absolute Error (MAE), and Mean Squared Error (MSE). Following a review of the LSTM model's graphical results, it was further enhanced by combining Autoencoder with LSTM, creating the Autoencoder LSTM (AELSTM) model. Next, a new hybrid model was introduced: Convolutional Neural Network-Autoencoder Long Short-Term Memory (HCAELSTM), designed to boost prediction accuracy. These models were trained on a one-year real-time solar power plant dataset for training and performance assessment. Ultimately, the hybrid HCAELSTM model surpassed the AELSTM model in terms of MAPE, MAE, and MSE. It excelled in MAPE scores for Daily Power Production, Peak Grid Power Production, and Solar Radiance, achieving low scores of 1.175, 2.116, and 1.592 respectively, demonstrating superior accuracy. The study underscores the importance of AI and ML, in particular, the hybrid model HCAELSTM, in enhancing the smart grid's ability to integrate renewable energy sources. The hybrid model excels at accurately forecasting key measurements, improving solar power generation efficiency within the smart grid system which also plays a key role in the broader shift toward the fourth energy revolution.

1. Introduction

In recent years, a significant global shift towards renewable energy sources has emerged, driven by concerns about the finite nature and environmental impact of conventional energy reserves like coal, oil, and gas. This urgency arises from the recognition that traditional energy sources contribute to greenhouse gas emissions, particularly carbon dioxide (CO2), exacerbating climate change. As the world's population grows and the

importance of sustainability becomes more widely acknowledged, the imperative to transition to more sustainable energy alternatives intensifies [1, 2]. Among renewable energy options, solar energy stands out for its exceptional eco-friendliness, sustainability, and widespread accessibility. Solar power offers a compelling alternative to traditional energy sources, paving the way for a greener and more sustainable future. By harnessing energy from the sun, solar power provides a virtually limitless and clean energy source free of greenhouse gas emissions. This not only helps mitigate climate change but also reduces our reliance on finite fossil fuels. Furthermore, once installed solar power systems require minimal maintenance, enhancing their appeal as a sustainable solution for meeting energy needs. ML algorithms are essential in the design of photovoltaic (PV) cells and in predicting energy output, which improves the efficiency and reliability of solar energy systems. Predictive modelling, classification, and optimization techniques aid in choosing the best materials and enhancing structural designs, resulting in more efficient and cost-effective PV cells. These algorithms also forecast solar radiation and power output, enabling better power plant operations, grid balancing, real-time unit dispatching, and trading. By analyzing historical weather data and environmental conditions, ML models provide precise short-term forecasts, reducing uncertainty and improving the quality of energy delivery to the grid. This dual application of ML in both the design and operational phases of PV systems highlights its critical role in advancing solar energy technology [2, 3].

Solar energy systems have a predictable payback time compared to traditional energy technologies like coal-fired power plants or natural gas generators, which can have indefinite payback periods due to variable fuel costs and ongoing operational expenses. This predictability stems from sunlight, the primary input of a solar energy system, being abundant and free once the system is in place [4, 5]. As a result, investors and energy users can more confidently project their return on investment, as the initial cost of solar panels and related equipment can be precisely amortized over time. This stability and assurance in an otherwise uncertain energy landscape increase the attractiveness of solar energy as a reliable and economically feasible choice for sustainable power generation [6]. However, the variability in sunshine intensity poses a significant challenge to maximizing solar energy utilization, as it can lead to fluctuations in power production and grid imbalances. Accurate forecasting of PV power generation is therefore essential for mitigating these oscillations and ensuring grid stability. With electricity playing a crucial role in driving economic growth and technological progress, the global energy demand continues to rise. This necessitates the expansion of both power generation and distribution networks, prompting governments and international bodies to implement policies favouring the widespread adoption of renewable energy sources [7–9].

In response to climate change, global warming, and escalating energy consumption concerns, governments are increasingly seeking sustainable and efficient energy solutions to balance environmental preservation with economic viability. The growing power demands from industrialization and urbanization underscore the need for a dependable and efficient power supply. Efficient power management is critical to avoid overproduction and the risk of blackouts due to the fluctuating generation of PV systems [10].

Research has utilized models like the Non-linear Autoregressive Exogenous Neural Network [11], LSTM-ARMA [12], and ARIMA [13] to estimate PV power generation, yet challenges remain due to solar irradiance variability. Factors such as sunlight angle, PV cell quality, module circuitry, solar cell properties, and weather significantly influence the electrical output of solar energy systems. Weather conditions like precipitation and cloud cover directly affect sunlight availability, impacting energy generation. Solar cell efficiency, material composition, and module circuitry determine overall system efficiency and reliability. Optimizing these parameters, including solar cell temperature control, is crucial for maximizing system efficiency and output [14]. Various reports highlight the importance of accurate PV power production prediction based on weather categorization to promptly address equipment and panel faults [15, 16]. Advanced models employing Deep Learning (DL) and ML, as examples of AI technologies, are essential for improving PV power production. These models account for various environmental conditions, enabling more precise high-output PV power forecasting [17]. Researchers have developed forecasting models specifically for short-term predictions, enhancing grid stability by providing reliable PV power output forecasts and improving solar energy system efficiency [18].

This study aims to enhance the accuracy of time series forecasting, we obtained a comprehensive dataset spanning one year of real-time data from a 100 MW solar plant, comprising Daily Power Production in KWh, Peak Grid Power Production in MW, and Solar Radiance in (MJ/m^2). Initially, we selected two distinct DL approaches, RNN and LSTM, based on existing literature. There were three sets of the dataset: training, testing, and validation, with 80% used for training and 20% reserved for final visualizations. Our graphical representations revealed that the LSTM model performed better than the RNN model, yielding more accurate forecasts, in comparable weather. Subsequently, we enhanced the LSTM model by incorporating an Autoencoder, resulting in the Autoencoder LSTM (AELSTM) model. Moreover, we introduced a novel hybrid model, CNN-Autoencoder LSTM (HCAELSTM), aimed at improving prediction accuracy. Evaluating the hybrid model's performance involved comprehensive analysis using metrics such as MAPE, MSE, and MAE. Comparison with the AELSTM, LSTM, and RNN models consistently showed the superior predictive

capabilities of the hybrid HCAELSTM model. Ultimately, our research aims to enhance the accuracy of time series forecasts by synergistically leveraging CNN and Autoencoder LSTM within a hybrid architecture. The study offers several significant contributions:

- Introduction of an innovative hybrid model, merging Convolutional Neural Networks (CNN) with an Autoencoder Long Short-Term Memory (AELSTM) framework. This approach leverages CNN's spatial feature extraction abilities and Autoencoder LSTM's proficiency in recognizing temporal relationships.
- Addressing a crucial gap by improving solar power generation systems efficiency in smart grid environments through the use of hybrid ML models, aiming to improve overall performance and accuracy.
- Demonstrating that the Hybrid HCAELSTM model outperforms standalone AELSTM, LSTM, and RNN models in forecasting solar power generation across various parameters. This superiority is consistently validated through rigorous evaluation using performance indicators such as MAPE, MAE, and MSE.
- Highlighting the immense potential of ML methods, especially the HCAELSTM hybrid methodology, through experimental studies and performance analyses, thereby improving knowledge of their efficiency in forecasting ideal measures for solar power production.
- Providing insightful information to stakeholders and decision-makers engaged in the design, installation, and operation of solar power production systems within smart grids. These revelations can inform tactics that maximize accuracy as well as effectiveness.

Section 2 of this paper provides an overview of existing research in the field. Section 3 offers a thorough exploration of the framework and methodology underpinning our proposed models, along with a comparative analysis. Following this, section 4 presents a case study focusing on the analysis of a solar power generation plant and the examination of collected data. In section 5, we present the results and engage in discussions, accompanied by comparisons and visual illustrations. The study is finally concluded in section 6.

2. Literature review

The global shift towards renewable energy sources has spurred extensive research into optimizing energy production from various locales. Studies have focused on identifying optimal regions for harnessing biomass, solar, wind, and hydrothermal energy. Among these, solar energy has seen significant advancements, particularly in rural areas, despite challenges such as weather variability, panel orientation changes, and system degradation that affect efficiency over time [19]. Recent advancements in forecasting techniques, particularly RNN models, have significantly improved PV power estimates. These innovations help smart grid operators make more informed decisions. Implementing ML approaches like RNNs enhances the accuracy and reliability of solar energy forecasting [20]. The study examines the efficacy of various ML/DL models for long-term solar energy forecasting, comparing them to traditional statistical methods. It finds that while ML/DL models improve prediction accuracy, long-term forecasting remains challenging and needs further research. The Random Forest model, in particular, predicted solar power generation with 50% better accuracy than univariate statistical models and 10% better accuracy than multivariate ML/DL models. [21]. ML models like artificial neural networks (ANN) and support vector machines (SVM) have shown superior performance in solar energy forecasting. These predictions help balance supply and demand, minimizing grid instability. Implementing these ML approaches enhances grid reliability [22]. Advanced ML frameworks, including hybrid models and DL architectures, leverage grid search optimization and probabilistic DL to further improve forecasting accuracy [23, 24].

Innovative models like residual multiscale recurrent neural networks (RM-RNN) and convolutional neural networks (CNNs) have been developed to enhance short-term power load and PV power generation forecasting, respectively [25, 26]. These AI-based approaches significantly address the challenges of renewable energy forecasting and optimize energy system performance [27, 28]. DL models such as long short-term memory (LSTM) networks have shown notable success in weather prediction and PV power forecasting, offering enhanced accuracy and scalability [29, 30]. The application of DL and ML methods in PV power output forecasting has gained traction, enabling accurate predictions based on seasonal and meteorological conditions [31, 32].

Various AI approaches, including DL and statistical models like ARIMA [33], hybrid models [14], Holt-Winters [34], and ANN [35], are commonly employed for PV power forecasting. Additionally, DL models such as Non-linear Autoregressive Exogenous Neural Network [11], LSTM-ARMA [36], Regression Neural Network [37], SARIMAX [38], and SARIMA [39] have been applied to improve forecasting precision. In [13] the

importance of short-term solar radiation forecasting for various operational aspects of solar PV power plants are discussed to improve energy delivery quality and reduce weather-dependent costs. It presents a new model for forecasting solar radiation and power output specifically for an 89.6 kWp solar PV power plant at Amity University Haryana (AUH) in northern India. The study compares this proposed model with the Smart Persistence and ARIMA models, highlighting its superior accuracy and reliability, as evidenced by lower RMSE and better Forecast Score (FS) for both 15 min and 30 min time horizons.

The rise of ML and DL models has addressed the variability in PV power generation forecasting [36, 40]. Researchers have explored time series models to predict PV power output based on seasonal and meteorological conditions [41–43]. DL models, particularly those that manage high noise levels and irrelevant data, have become popular for PV production forecasting [44]. LSTM's advanced memory mechanism allows it to retain previous knowledge effectively, achieving remarkable accuracy in time-series datasets [45]. Compared to other time-series forecasting models like Linear Regression, ARIMA, SARIMA, ARIMAX, and SARIMAX, LSTM demonstrates the lowest error rate in forecasting PV power production output [46]. The hybrid CNN-LSTM model has emerged as a superior predictor for solar energy variables, outperforming traditional ANN and RNN models [47]. Despite the potential for dataset expansion, challenges remain in the availability and quality of diverse data sources. Similarly, in [31] introduces a DL framework combining CNN and LSTM for short-term electric load forecasting of individual residential customers is introduced. The hybrid CNN-LSTM model effectively utilizes CNN layers for feature extraction and LSTM layers for sequence learning. Tested on data from the Smart Grid Smart City (SGSC) project, the model achieved an average MAPE of 40.38%, outperforming the LSTM-based model's 44.06%. Additionally, the CNN-LSTM model showed significant improvements in forecasting accuracy for one, two, and six look-forward time steps. Clustering analysis based on power consumption behavior suggested that grouping users and training with larger datasets could further enhance prediction accuracy. Additionally, a hybrid framework combining CNN, A-LSTM network, and Auto-Regression model accurately forecasts power generation from multiple renewable energy sources, surpassing advanced models like ANN and decision trees [48].

In [49], ML approaches for solar energy forecasting were enhanced using a hybrid model that integrates LSTM networks and autoencoders. This model addresses challenges such as data noise and uncertainties in weather conditions, significantly improving day-ahead solar plant output predictions. By leveraging renewable energy data, the model achieves higher forecasting accuracy. Similarly in [50], ML technique, particularly the Autoencoder LSTM model, showed superior accuracy in forecasting solar energy parameters compared to LSTM and CNN LSTM models. The study underscores the importance of AI and ML in enhancing solar energy forecasting, which is critical for optimizing smart grid performance. The use of advanced ML models significantly improves prediction precision, contributing to better power generation capacity and reduced energy losses. In [51, 52], ML models were utilized to forecast PV system power output, highlighting their critical role in improving solar energy predictions. These approaches are essential for enhancing forecasting accuracy and optimizing the management of solar power resources. Effective ML models significantly contribute to better planning and integration of solar energy in power grids. This study highlights the importance of advanced ML approaches for solar energy forecasting, specifically using the hybrid Autoencoder LSTM model, which outperformed both LSTM and Bi-LSTM models in accuracy of solar power generation data. These findings emphasize the significant potential of hybrid ML models in enhancing renewable energy integration into smart grids, leading to more efficient and accurate predictions [53]. Similarly, the hybrid method combining LSTM neural networks and autoencoders demonstrated superior performance in solar energy forecasting compared to existing models. Effective AI-based ML models are crucial for enhancing prediction accuracy in solar power forecasting, optimizing smart grid integration, and improving overall energy management [54]. In many developed countries, photovoltaic solar power is a major and cost-effective renewable energy source, but its variability poses challenges for accurate forecasting. Accurate PV power prediction is crucial for the secure and efficient operation of solar power systems. The LSTM autoencoder (AE) model has demonstrated superior performance over benchmark deep learning methods in forecasting PV power, highlighting the importance of advanced ML approaches for improving forecast accuracy, as evidenced by improved MAE, RMSE, and R-squared metrics in a 23.40 kW PV power plant dataset from Australia [55].

3. Proposed framework/methodology

In The study involves developing and evaluating ML models for predicting the performance and power generation of a solar power plant using three key parameters: Daily Power Production in KWh, Peak Grid Power Production in MW, and Solar Radiance in MJ/m^2. The data is divided into 80% for training, testing, and validation, with the remaining 20% used for prediction and evaluation. After experimenting with various models, including statistical, conventional, and different ML methods like ARIMA, SVM, and RF, the study

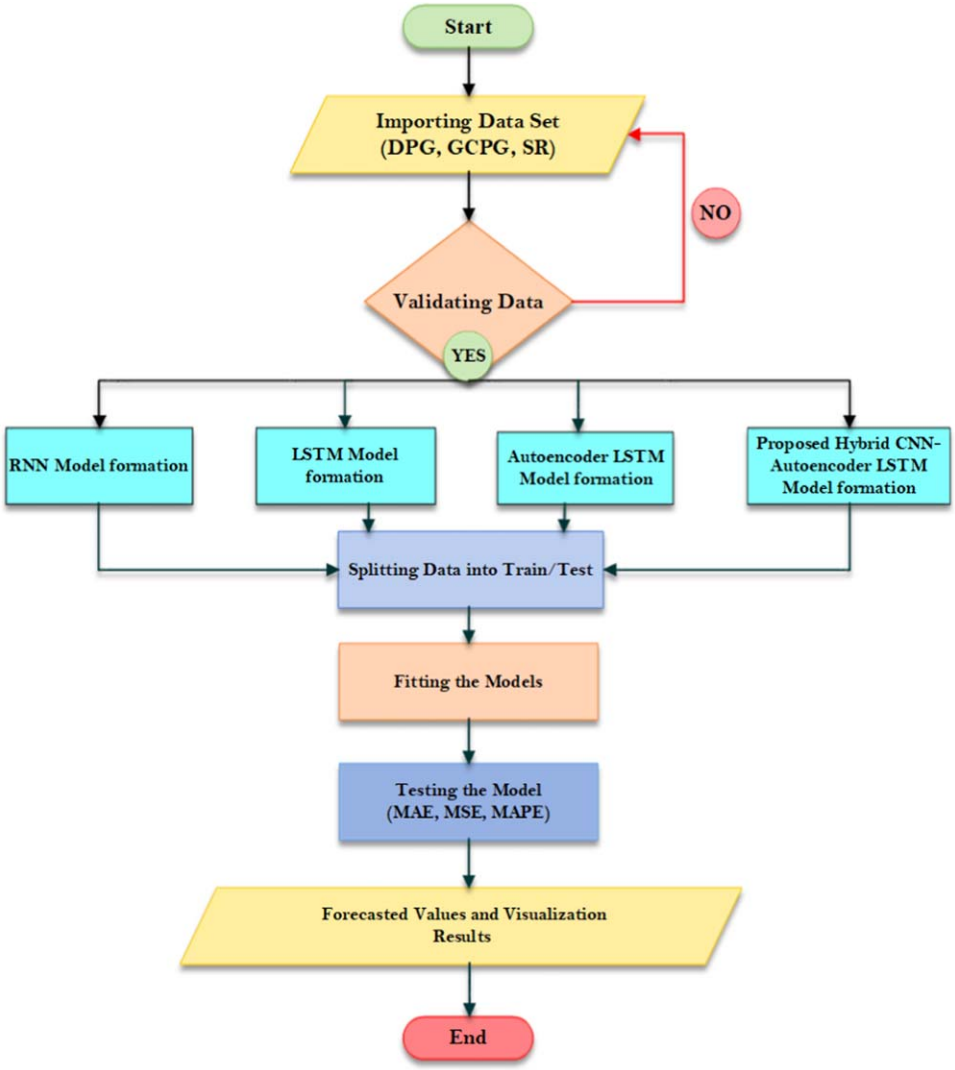

Figure 1. Process for visualization results through RNN, LSTM, AELSTM and Hybrid HCAELSTM.

found that LSTM and RNN performed the best. Further enhancements were made to LSTM by integrating an Autoencoder, resulting in an Autoencoder LSTM (AELSTM) model, and a novel hybrid model combining CNN, Autoencoder, and LSTM (HCAELSTM) to improve prediction accuracy.

The process starts by validating the data and dividing it into training and testing sets. The models are evaluated in terms of R^2, MAPE, MSE, and MAE. Visualizations of the predictions and errors are generated based on the trained models, providing a comprehensive overview of the predicted outcomes. Operators of solar power plants may find these projections useful in making decisions about pricing strategies, efficient energy system planning, reliability of the system, and other important design elements. In comparative evaluations, the hybrid HCAELSTM model exhibited lower MAPE, MSE, and MAE and higher R^2 values, indicating superior prediction accuracy for real-time data compared to other models.

The study article provides a thorough comparison of the models, and figure 1 shows a detailed flowchart that outlines the whole process along with the models' graphical results. In the subsections that follow, the models' mathematical components and structural details are covered in detail.

3.1. Structure of RNN

Figure 2 shows the most basic form of an RNN cell, which faces challenges such as vanishing and exploding gradients over lengthy sequences. These problems occur because the cell struggles to maintain long-term dependencies. The gradient of back-propagated tends to decline with length of sequence, preventing the model from updating the weights effectively. On the other hand, excessively large gradients can lead to instability and unreliable weight matrices. These issues arise from the inability of RNN cells to handle unsolvable gradients, which impede the recognition and consideration of long-term connections.

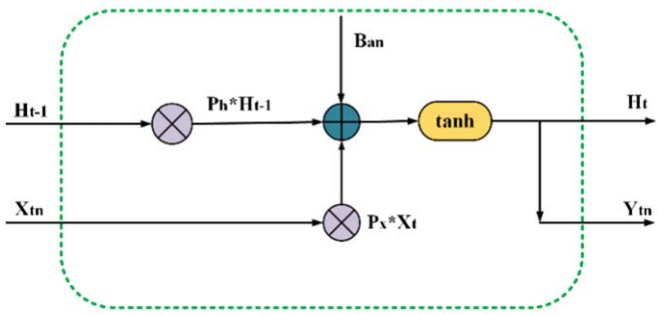

Figure 2. Structure of RNN.

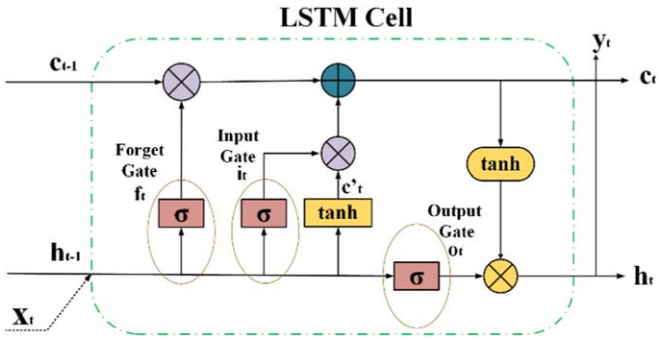

Figure 3. Structure of LSTM.

$$H_{t-1} = \sigma(P_h * H_{t-1} + P_x * H_t + B_a) \tag{1}$$

$$Y_t = \tan h(P_o * H_t + B_o) \tag{2}$$

In equation (1) also in (2), of the RNN (H_{t-1}) and (H_t) represent the previous and current hidden states, respectively. The RNN cell is able to remember information as time passes because of these hidden states. At time (t) step, (X_t) and (Y_t) symbolize the input and output, respectively. The weight matrices (P_h), (P_x), and (P_o), along with the bias vectors (B_a) and (B_o), control the transformation and response of the state of hidden.

The current (H_t) state of hidden is influenced not just by the previous time step's state of hidden H_{t-1} but also by the current (X_t) input. This dependency allows the model to combine past information with the current input to produce the new state. The presence of feedback loops in the RNN cell plays a key role by linking the cell's among the current state and future state. These are important connections because they enable the model to integrate information from the past while updating the cell's current state. The sigmoid function (denoted as σ is used as the activation function for the state of hidden, while the tangent function (represented as tanh) hyperbolic serves as the activation function for the output. These functions are indicated by their respective symbols and play distinct roles in the model's operations.

3.2. Structure of LSTM

A kind of recurrent neural network (RNN) called the Long Short-Term Memory (LSTM) network was created to solve two significant problems with conventional RNNs: the vanishing gradient problem and the inflating gradient problem. The input, forget, and output gates are only a few of the gates that are introduced by Sepp Hochreiter and Jürgen Schmidhuber's LSTM to control the information flow inside the network. In contrast to traditional feed-forward neural networks, which can only process information in a single direction, long short-term memory (LSTM) networks can function on both input and internal state spaces. Because of their adaptability, long sequence learning machines (LSTMs) are ideally suited for jobs that need sequential data retention. Figure 3 illustrates the structure of an LSTM cell, which is made up of the input gate, forget gate, output gate, and memory cell, among other essential parts. Together, these elements allow the network's information flow to be updated and controlled in a selective manner, which helps LSTMs recognize long-range relationships in sequential data.

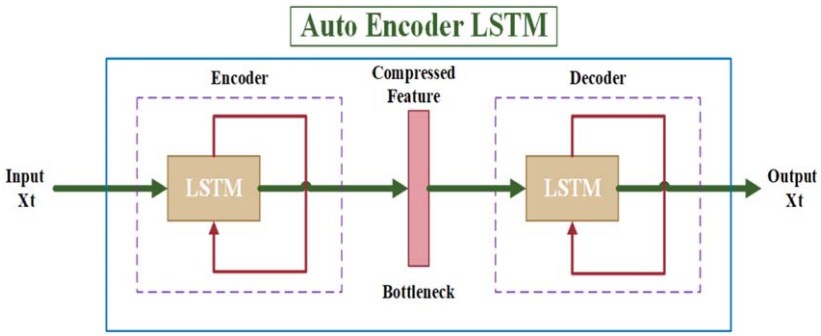

Figure 4. Structure of autoencoder LSTM.

The forget gate f_t in equation (3) of an LSTM network uses a sigmoid function (σ) to combine the previous hidden state h_{t-1}, current input x_t, and weighted sum (W_f) with a bias term to decide which information to retain or discard. This selective filtering is crucial for maintaining essential long-term memory and capturing dependencies in sequential data.

$$f_t = \sigma\{W_f(h_{t-1},\ x_t)\} \tag{3}$$

In an LSTM network, the input gate I_t decides which parts of the current cell state (f_t) to update. An input layer gate and a tanh layer make up its two components. The input gate layer uses a sigmoid function (σ) to select values to update, while the tanh layer creates new candidate values (C'_t) to add to the cell state. This process is shown in equations (3) and (4).

$$I_t = \sigma\{W_i(h_{t-1},\ x_t)\} \tag{4}$$

$$C'_t = \tanh\{W_c{*}(h_{t-1}, x_t)\} \tag{5}$$

In an LSTM network, the cell state (C_t) manages information flow over time by integrating outputs from the forget gate (f_t), input gate (I_t), previous state of cell (C_{t-1}), and candidate state of cell (C'_t). It uses element-wise operations to selectively preserve useful information and discard irrelevant data, thus ensuring the network efficiently retains important data.

$$C_t = (f_t{*}C_{t-1}) + C_t{*}C'_t \tag{6}$$

In an LSTM network, the output (O_t) gate chooses the information from the current state of cell (C_t) should be included in the state of hidden (h_t). According to equation (7), the cell state (C_t) is activated using tanh and then multiplied by the output O_t gate. This process allows only relevant information to pass to the hidden state, aiding the network in capturing meaningful features and patterns in the data.

$$O_t = \sigma\{W_o.(h_{t-1}, x_t) \tag{7}$$

$$h_t = O_t{*}\tanh(C_t) \tag{8}$$

The output gate enables the flow of processed data to subsequent layers in the network, supporting the propagation of information and generation of meaningful outcomes. The data processed by the output gate serves as input for the next layer, whether it's another LSTM or another type of neural network. This continuous flow of information across layers improves the network's ability to learn complex patterns and make precise predictions or classifications.

3.3. Structure of autoencoder LSTM

The Autoencoder LSTM combines Autoencoders with LSTM networks to create a robust neural network framework, as shown in figure 4. Autoencoders compress input data into a smaller representation and then reconstruct it, while LSTM cells track time-based correlations in sequential data. In this setup, LSTM cells in the encoder section manage the order of input and produce an encoding, reducing data dimensionality. Meanwhile, LSTM cells in the decoder aim to replicate the input sequence and minimize reconstruction errors. Training involves providing input sequences and using a loss function such as MSE or binary cross-entropy. Once trained, Autoencoder LSTM can compress and reconstruct input sequences, retaining important information in lower dimensions. This framework is useful for tasks like serial prediction, anomaly detection, and feature extraction from data in sequence. Autoencoder LSTM stands out in data analysis, pattern recognition, and data reconstruction, making it a powerful tool across various fields.

Autoencoders (AE) are commonly used in unsupervised learning for learning representations. They consist of four key components: Encoder, Bottleneck, Decoder, and Reconstruction Loss. The input data is compressed by the encoder and reduces its dimensionality, while the Bottleneck creates a compact data representation. The input is subsequently reconstructed by the decoder using this compressed form, and the Reconstruction Loss function works to minimize errors in the reconstruction process. By accurately reconstructing time series data, Autoencoders enable efficient representation learning and data compression, which are important for effective time series predictions.

Equations (9) and (10) represent encoding and decoding, respectively.

$$t_i = f\,(w_t.x_i + b_t) \tag{9}$$

$$y_i = g\,(w_y.t_i + b_y) \tag{10}$$

Where sigmoid functions are denoted by $(\cdot)$ and $(\cdot)$, and w_t, w_y represent weights and b_t, b_y denote biases.

In equation (11), the hidden state f_t of the autoencoder is computed by combining the input x_t , additional data z_t , and the previous hidden state h_{t-1} using weights and biases. The computation becomes nonlinear when a sigmoid function is used, while the candidate cell state C_t combines inputs, additional data, and the previous state of hidden, applying a hyperbolic tangent function.

$$f_t = \sigma(w_{f1}.x_t + w_{f2}.z_t + wf_3.h_{t-1} + b_f) \tag{11}$$

$$i_t = \sigma(w_{i1}.x_t + w_{i2}.z_t + w_{i3}.h_{t-1} + b_i) \tag{12}$$

In equation (14), the previous cell state C_{t-1} is combined with the candidate state of cell C'_t based on the forget gate f_t and input gate i_t. Equation (15) determines the output o_t gate by taking average between inputs and the current hidden state using the sigmoid function. The final hidden state h_t is obtained from the cell state C_t using the tan h function. These equations, along with encoding and decoding processes, are key to the Autoencoder's ability to regenerate data.

$$C'_t = \tanh(w_{c1}.x_t + w_{c2}.z_t + w_{c3}.h_{t-1} + b_c) \tag{13}$$

$$C_t = f_t.C_{t-1} + i_t.C'_t \tag{14}$$

The representation z_t captures traffic movement features and utilizes biases (b_f, b_i, b_c, b_o) and weights (W_f, W_i, W_c, W_o) for calculations. The forget gate processes the inputs x_t, z_t, and the previous hidden state h_{t-1} through a sigmoid function (σ). Cell states C_t and C_{t-1} adjust each time step, while the output gate, selects key data that the tanh function then uses to analyze the cell state.

$$o_t = \sigma(w_{o1}.x_t + w_{o2}.z_t + w_{o3}.h_{t-1} + b_o) \tag{15}$$

$$h_t = o_t.\ \tanh(C_t) \tag{16}$$

3.4. Structure of convolutional neural network

The architecture of a Convolutional Neural Network (CNN) is illustrated in figure 5 and is defined by its stacked layers and kernel sizes. In the early layers, the input data undergoes convolution and pooling operations, extracting complex features that are then fed into the fully connected layer for classification. CNNs excel in capturing layered features from images, as well as one-dimensional sequential and two-dimensional input data.

Convolution layers are essential for identifying spatial features by applying convolutional kernels to input data. Activation layers, typically using functions like ReLU, provide the model non-linearity to help it recognize intricate patterns and correlations in the data.

Pooling layers follow the convolution layers and are used to downsample the feature maps, reducing their dimensionality while retaining important information. Pooling helps in reducing computational complexity and enhances the model's robustness against minor variations in the input data. By combining these layers, CNNs effectively integrate local and global features, demonstrating their adaptability across various applications such as solar energy forecasting, where CNN's convolution processing improves time series analysis.

$$z = \sigma(W^*x + b) \tag{17}$$

In equation (17), z represents the output feature map generated by applying a convolution operation (W^*x) between the filter weights and the input data. This operation is followed by an activation function σ, which introduces non-linearity into the model.

$$z' = p(z) \tag{18}$$

In equation (18), the output of the pooling layer z' is calculated from the input feature map z. The pooling operation, denoted as p, condenses the dimensions of the feature map, helping to reduce computational complexity while retaining important information.

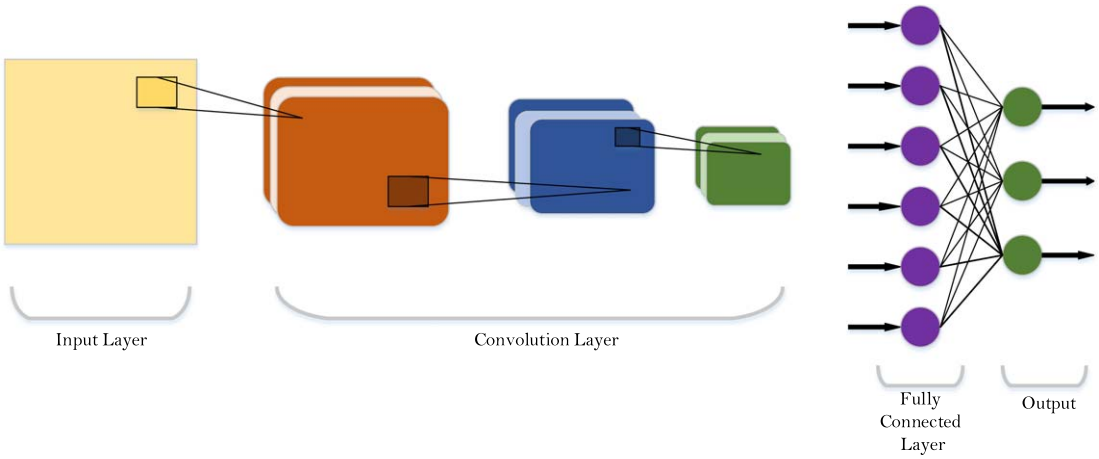

Figure 5. Standard convolutional neural network (CNN) architecture.

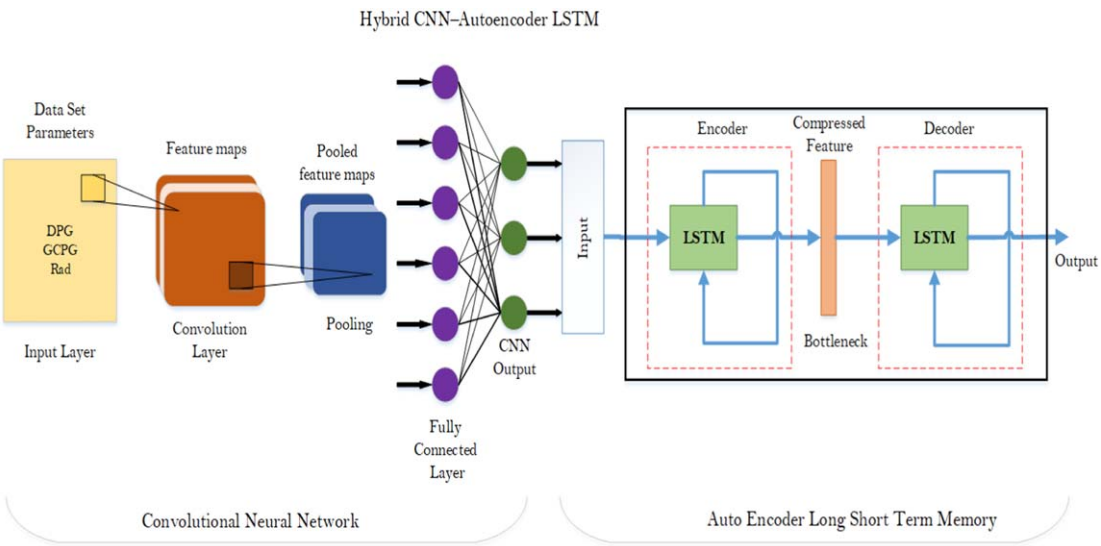

Figure 6. Hybrid CNN with AELSTM model.

3.5. Hybrid CNN—autoencoder LSTM

The proposed hybrid model architecture combines Convolutional Neural Networks (CNN) and Autoencoder Long Short-Term Memory (AELSTM) networks as depicted in figure 6 to enhance forecasting accuracy and effectiveness. The model begins by processing input data through the CNN architecture, which includes an input layer and hidden layers such as convolution, dropout, pooling, and ReLU layers. Specifically, a pair of convolution layers with the ReLU activation function is followed by a dropout layer. CNNs are adept at extracting spatial features from data, making them well-suited for tasks like image recognition. In this hybrid model, the CNN layers capture important features from the input data related to solar power generation, such as patterns in solar plant key parameters.

Once the CNN layers have extracted these features, they are passed on to the AELSTM architecture. LSTM networks excel at capturing temporal dependencies in sequential data. By integrating AELSTM, the model can capture both spatial as well as temporal patterns in the input data, enhancing its ability to make accurate predictions. The AELSTM architecture processes the features extracted by the CNN layers by encoding them into a compact representation while preserving important temporal relationships. This encoded representation is then decoded to generate forecasts for the desired output parameters.

The hybrid model merges the spatial feature extraction abilities of CNN with the temporal modeling strengths of AELSTM. This integration allows for a comprehensive analysis of the input data, leading to more

accurate predictions and superior performance in forecasting solar power generation parameters compared to traditional models.

3.6. Comparison with other conventional models

In time series forecasting, ARIMA (AutoRegressive Integrated Moving Average) model [33], while popular for their simplicity and interpretability, have significant limitations. ARIMA models require the data to be stationary, meaning they may struggle with complex patterns, non-linearities, and seasonality present in real-world datasets. Additionally, ARIMA models do not effectively handle large datasets or multiple variables, leading to a move towards more flexible and powerful ML models like Support Vector Machines (SVM) [22] and Random Forests (RF) [40]. SVM can capture non-linear relationships, while RF can manage large datasets and multiple variables better. However, these ML models still have limitations, such as difficulty in capturing long-term dependencies and requiring feature engineering, prompting the shift to DL models like Recurrent Neural Networks (RNN) and Long Short-Term Memory (LSTM) networks. LSTM networks, designed to overcome the vanishing gradient problem of RNNs, can capture long-term dependencies and sequential patterns in time series data. However, LSTMs still face limitations, such as high computational cost and difficulty in capturing spatial patterns. To address these issues, the Autoencoder LSTM model is introduced, which can effectively reduce dimensionality and capture complex temporal dependencies. Despite this advancement, there is still room for improvement in handling spatial-temporal features comprehensively, leading to the development of hybrid models that combine Convolutional Neural Networks (CNN) with Autoencoder LSTM. This hybrid approach leverages the strength of CNNs in capturing spatial features and the capability of LSTM in modelling temporal sequences, resulting in superior performance and better forecasting accuracy compared to traditional and standalone models.

The superior performance of the Hybrid CNN with Autoencoder LSTM (HCAELSTM) model in forecasting tasks can be attributed to the synergistic strengths of Convolutional Neural Networks (CNNs) and Autoencoder Long Short-Term Memory (LSTM) networks. CNNs are highly effective at capturing spatial patterns and local features within the data. When applied to time-series data, CNNs can identify important patterns over time, such as seasonality, trends, and periodic fluctuations. Through multiple convolutional layers, CNNs can extract hierarchical features, where higher layers represent more abstract and complex patterns. This is particularly useful for capturing intricate relationships in the data that might be missed by simpler models. Moreover, CNNs can reduce the dimensionality of the data through pooling operations, which helps in reducing computational complexity and overfitting, retaining the most important features while discarding redundant information. On the other hand, Autoencoder LSTMs combine the capabilities of LSTMs and autoencoders to enhance the model's ability to capture temporal dependencies and reduce noise. LSTMs are designed to capture temporal dependencies and long-range correlations in sequential data, making them well-suited for time-series forecasting as they can remember important information over long periods and forget irrelevant data. By incorporating autoencoders, the model can effectively compress the input data into a lower-dimensional latent space and then reconstruct it, capturing essential temporal features and reducing noise. This helps in handling non-stationary time-series data where statistical properties change over time, maintaining performance even when the underlying data distribution changes.

In summary, the HCAELSTM model combines CNN and Autoencoder LSTM to enhance time-series forecasting. CNN layers identify and extract significant features, capturing complex patterns. The autoencoder LSTM component reduces noise and dimensionality, retaining essential temporal features. The LSTM layers accurately model temporal dependencies, resulting in robust and precise forecasts. This integration allows HCAELSTM to outperform existing models, particularly in handling complex, noisy, and non-stationary time-series data, leading to improved forecasting accuracy and consistency.

4. Case study

4.1. Solar plant's structure

The Zhenfa Energy Group Solar PV Park is a significant renewable energy project located in Punjab, Pakistan. Developed and owned by Zhenfa New Energy, it boasts a capacity of 100 megawatts (MW) and covers an impressive area of 650 acres. Operational since April 2022, the project generates an impressive 188,427.6 megawatt-hours (MWh) of electricity annually, providing sustainable power to approximately 50,000 households. Key components of the project include 229,885 PV modules supplied by Zhangjiagang SEGPV, each with a capacity of 435 W, and Sungrow Power Supply's SG 630 MX inverters. Zhenfa New Energy, headquartered in Wuxi, Anhui, China, focuses on investment, development, and operation of PV Power Projects.

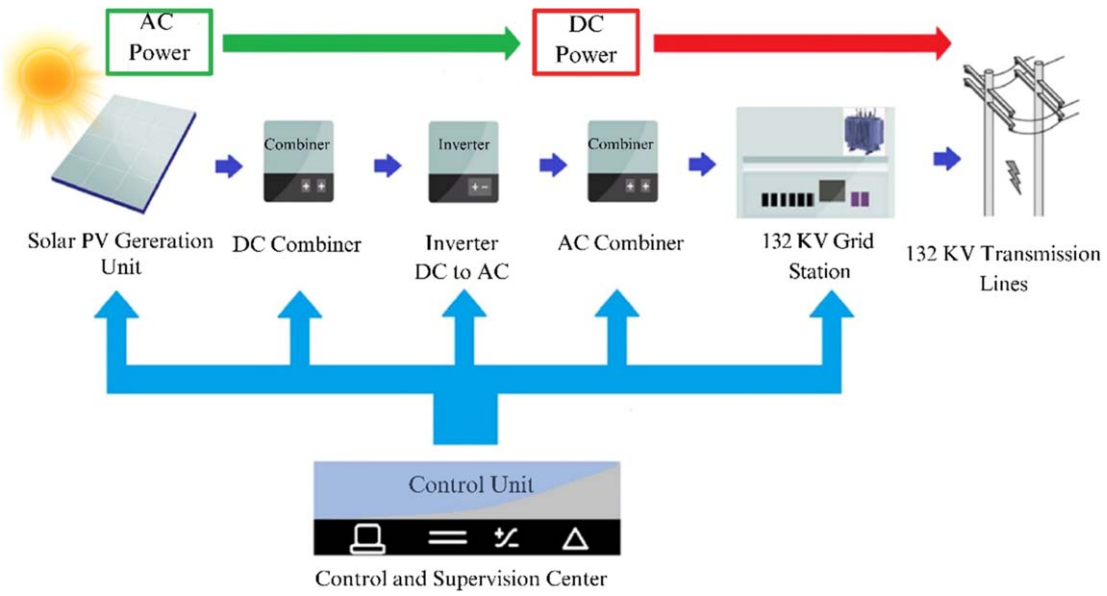

Figure 7. Single line diagram to express the structure of solar plant.

The establishment and operation of the Zhenfa Energy Group Solar PV Park mark a significant advancement for renewable energy in Pakistan. By generating a substantial amount of electricity, this solar park helps reduce Pakistan's dependence on fossil fuels, thereby aiding the country's efforts to combat climate change. Its successful implementation demonstrates the feasibility and promise of large-scale solar projects in the region, setting a crucial milestone for the green energy sector in Pakistan. This initiative not only contributes to sustainable development goals but also underscores the potential for widespread adoption of solar power as a clean and efficient energy source in the country.

Notably, figure 7 illustrates the solar plant's construction and offers pertinent insights into the data garnered from this remarkable facility. Based on the provided figure, the data collection process for solar power forecasting involves monitoring and recording three key parameters: Daily Power Production, Peak Grid Power Production, and Solar Radiance. The unit control and supervision center, incorporating SCADA and data acquisition device, ensures efficient data collection process within the solar PV plant. Daily Power Production represents the total amount of electrical energy generated by the Solar PV Generation Unit over the course of a day. The data is collected from the DC combiner, inverter, and AC combiner units, ensuring accurate measurement of the daily power output after converting DC to AC power and before the electricity is transmitted to the grid. Peak Grid Power Production measures the highest power output achieved by the solar PV system during the day, with data collected from the 132 KV Grid Station, which receives the AC power from the solar plant and records peak power values. This metric is crucial for understanding the maximum capacity and efficiency of the solar PV system. Solar Radiance data is collected from sensors installed on the Solar PV Generation Unit, capturing the intensity of sunlight received by the solar panels. This parameter is critical for correlating power production with sunlight availability.

To ensure the dataset's quality and suitability for training the ML models, several data preprocessing steps were undertaken using the one-year real-time dataset from the Zhenfa Energy Group Solar PV Park, which consists of three parameters: Daily Power Production, Peak Grid Power Production, and Solar Radiance. The initial step involved handling missing values. Any missing data points were identified and addressed using interpolation techniques or by filling them with mean or median values, depending on the nature and distribution of the missing data. Next, outliers were detected using statistical methods such as the Z-score method and IQR (Interquartile Range) and were either corrected if they resulted from sensor errors or removed if they represented anomalous events that did not reflect typical conditions. Normalization was then applied to ensure all features had a similar scale, which is crucial for improving the convergence rate of ML algorithms. Min-max scaling was utilized to transform the features into a common scale, ensuring uniformity in the data. To enhance the predictive power of the model, additional features were derived. Time-based features such as the day of the week and seasonal indicators were created to capture temporal patterns in solar power generation. These engineered features aimed to provide the model with more context about the data. The dataset was divided into training, validation, and test sets to evaluate the model's performance effectively. The training and validation set consisted of data from the first ten months, and the test set comprised the last two month. This

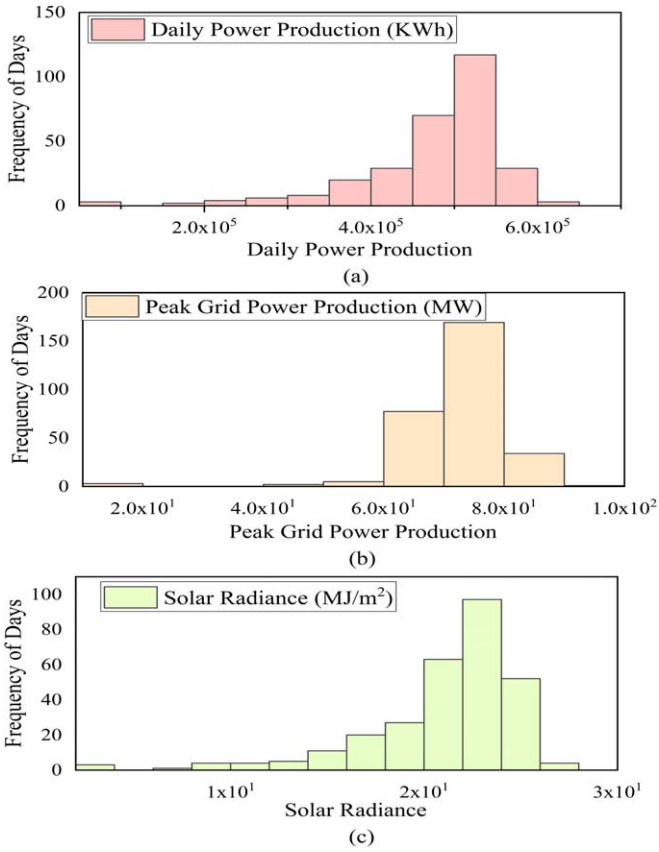

Figure 8. (a)–(c) Analysis of data using a histogram for parameters of solar plant.

chronological split ensured that the model was tested on unseen data, providing an unbiased assessment of its performance. To further enhance the robustness of the model, data augmentation techniques were applied. This involved generating synthetic data points by slightly varying the input parameters within realistic ranges. These variations simulated different environmental conditions, thereby improving the model's ability to generalize across diverse scenarios. By following these preprocessing steps, the dataset was meticulously prepared for training our hybrid model, HCAELSTM (CNN with Autoencoder LSTM). This preparation ensured high-quality input data, thereby improving the accuracy and reliability of the solar power forecasting models.

4.2. Data analysis

A useful analytical tool for analyzing a dataset's properties, a histogram provides information on the distribution, central tendency, and spread of the data. It facilitates the identification of any normal distribution by showing the frequency range of the data points. Furthermore, histograms compute significant statistical values such as the data's mean, median, and variability. They make evident patterns that simplify the process of comprehending the distribution of the data. This makes it easier to compare several datasets directly and reveals hidden patterns in the raw data. A histogram arranges data in a way that is easily readable by the eye, much like a pie chart.

The histogram labelled 'Daily Power Production in kWh' in figure 8(a) shows the trend of daily power production. The horizontal dimension displays the power produced in kilowatt-hours (kWh), with a range of 0 to 7.0×105 kWh. The frequency of each power producing quantity is measured on the vertical dimension, ranging from 0 to 150 occurrences.

The histogram titled 'Peak Grid Power Production in MW' in figure 8(b) shows the frequency of the grid's highest power production. The horizontal dimension splits the maximum power production values into intervals from 0 to 1.0×10^2 megawatts (MW), while the vertical axis spans from 0 to 200 occurrences. This graph illustrates the frequency of each interval to demonstrate trends in maximum grid-based power levels over time.

The histogram labelled 'Solar Radiance (MJ/m^2)' in figure 8(c) displays observations of solar radiation. The horizontal dimension operates from 0 to 3.0×10^1 MJ m^{-2}, representing solar radiance levels, while the vertical dimension shows the frequency of each radiance value from 0 to 100. The distribution of radiance readings is

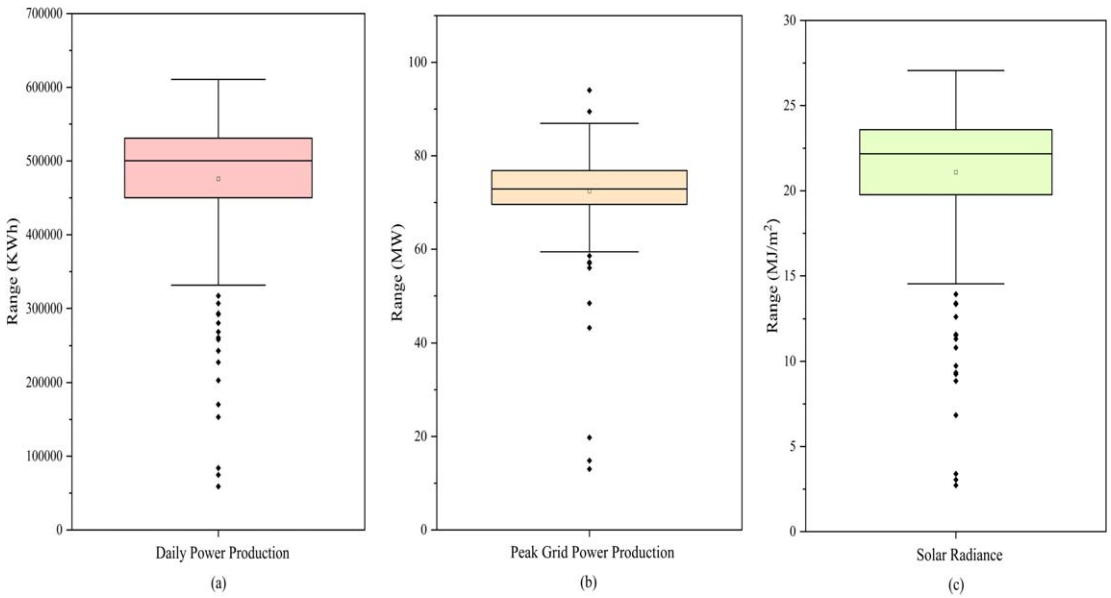

Figure 9. (a)–(c) Analysis of data using box plot for parameters of solar plant.

depicted by the form of the histogram, where a box to the right skew denotes higher scores and to the left skew predicts lower scores. A symmetrical form suggests that the radiance levels are distributed evenly.

As shown in figures 9(a)–(c), box plots are a helpful tool for summarizing and graphically representing data distributions. They provide insightful information on three particular traits taken from a noteworthy dataset of solar power plants. Both the dominant trend and the variation of these features are effectively communicated by each of the boxes plot.

The distribution of the daily power production data is displayed on the *y*-axis of a box plot labeled 'Daily Power Production in kWh' in figure 9(a). The data ranges from 0 to 7×10^5 kWh. The data is divided into parts by the quartiles: The lowest 25% of the data (3.4×10^5 to 4.5×10^5 kWh) is represented by Q1, the median (4.5×10^5 to 5×10^5 kWh) is represented by Q2, the highest 25% of the data (5×10^5 to 5.3×10^5 kWh) is covered by Q3, and the top 1% of the data (5.3×10^5 to 6.1×10^5 kWh) is included in Q4.

The box plot titled 'Peak Grid Power Production in MW' in figure 9(b) shows the highest power generation data on the *y*-axis, which ranges from 0 to 1×10^2 MW. Once more, the data are divided by the quartiles: Q1 covers the lowest 25% of data, from 6×10^1 to 7×10^1 MW; Q2 is the median (7×10^1 to 7.3×10^1 MW); Q3 covers the highest 25% of data, from 7.3×10^1 to 7.8×10^1 MW; and Q4 covers the top 1% of data, from 7.8×10^1 to 8.8×10^1 MW.

Lastly, the box plot labeled 'Solar Radiance in MJ·m−2' in figure 8(c) illustrates the distribution of radiance values on the *y*-axis, which spans from 0 to 3.0×10^1 MJ m^{-2}. The data are shown by the quartiles: Q1 comprises the lowest 25% of data, ranging from 1.4×10^1 to 2.0×10^1 MJ m^{-2}. Q2 comprises the middle 50% of data, ranging from 2.0×10^1 to 2.25×10^1 MJ m^{-2}. Q3 covers the highest 25% of data, from 2.25×10^1 to 2.35×10^1 MJ m^{-2}, and Q4 includes the top 1% of data, from 2.35×10^1 to 2.7×10^1 MJ m^{-2}.

The practical implications of improved forecasting accuracy for Daily Power Production (kWh), Peak Grid Power Production (MW), and Solar Radiance (MJ/m^2) has significant implications for solar power plants. Enhanced daily power production forecasts optimize resource allocation and panel adjustments, leading to efficient storage use and reduced operational costs. Accurate peak grid power production predictions help balance supply and demand, minimizing grid instability and enhancing reliability. Improved solar radiance forecasts refine solar energy integration into the grid, reducing curtailment and increasing utilization. These accurate forecasts are crucial for plant performance, maintenance, revenue estimation, grid stability, energy pricing, and renewable energy integration, ultimately optimizing efficiency, sustainability, and reliability in solar energy generation.

Moreover, these accurate forecasts provide critical data for grid stability by allowing for precise scheduling of power generation and distribution, preventing grid overloads, and reducing the need for costly peaking power plants. This, in turn, supports the development and expansion of solar power infrastructure by making solar projects more attractive to investors due to the reduced financial risk and predictable returns. The improved forecasting capabilities also facilitate the incorporation of hybrid energy systems that combine solar power with other renewable sources, optimizing the overall energy mix and enhancing system reliability and efficiency.

Table 1. MAPE and RMSE results comparison between ARIMA, SVM, RF, LSTM and HCAELSTM.

Parameter	ARIMA		SVM		RF		LSTM		HCAELSTM	
	MAPE	RMSE	MAPE	RMSE	MAPE	RMSE	MAPE	RMSE	MAPE	RMSE
Daily Power Production	8.177	0.6057	5.287	0.5281	4.563	0.4652	2.71	0.3124	1.175	0.1276
Peak Grid Power Production	6.93	0.3492	4.42	0.2929	3.601	0.2683	2.43	0.1964	2.116	0.0803
Solar Radiance	10.64	0.5160	6.834	0.4697	6.084	0.3963	3.36	0.2328	1.592	0.1286

Table 2. MAE and MSE results comparison between ARIMA, SVM, RF, LSTM and HCAELSTM.

Models	Daily power production		Peak grid power production		Solar radiance	
	MAE (KWh)	MSE	MAE (MW)	MSE	MAE (MJ/m^2)	MSE
ARIMA	0.9389	0.3669	0.5568	0.122	0.6724	0.2663
SVM	0.7437	0.2789	0.4519	0.0858	0.5298	0.2207
RF	0.554	0.2165	0.3285	0.072	0.3968	0.1571
LSTM	0.2223	0.0976	0.1219	0.0386	0.1618	0.0542
HCAELSTM	0.0782	0.0162	0.0406	0.0064	0.0750	0.0165

The HCAELSTM model's ability to deliver accurate predictions for these key parameters plays a crucial role in advancing smart grid operations. It supports innovative grid management techniques such as demand response, distributed generation, and real-time energy trading, contributing to a more resilient and adaptable energy infrastructure. By enhancing the operational and financial performance of solar power plants and promoting the integration of renewable energy sources, this advancement aligns with global efforts to reduce dependence on fossil fuels and mitigate climate change, driving the transition to a sustainable energy future.

The results derived from each of the four models are shown graphically in section 5 that follows.

5. Results and discussion

In this study, we collected a comprehensive dataset over a year from a solar power plant, including real-time records of three key parameters: 'Daily power production in kWh,' 'Peak Grid power production in MW,' and 'Solar Radiance in MJ/m^2.' These variables were used to forecast the next year's 'Daily Power Production, Peak Grid Power Production, and Solar Radiance.' Our goal was to develop ML models for future predictions based on this dataset, following an extensive literature review. We initially compared various traditional methods, including the classical statistical model Autoregressive Integrated Moving Average (ARIMA) [13, 33], ML approaches like Support Vector Machine (SVM) [22] and Random Forest (RF) [40], and DL techniques such as Long Short-Term Memory (LSTM) and our proposed Hybrid CNN with Autoencoder LSTM (HCAELSTM). Our comparison of time series prediction methods for solar power plant parameters showed a clear improvement in accuracy from traditional statistical models to advanced DL techniques. Starting with ARIMA, we found that ML approaches like SVM had lower errors. For the Daily power production parameter, The ARIMA model exhibited the highest errors with a Mean Absolute Percentage Error (MAPE) of 8.177 and a Root Mean Squared Error (RMSE) of 0.6057. The Support Vector Machine (SVM) model improved upon ARIMA, achieving a MAPE of 5.287 and an RMSE of 0.5281. The Random Forest (RF) model further reduced the errors, with a MAPE of 4.563 and an RMSE of 0.4652. Moving to DL methods, the Long Short-Term Memory (LSTM) model showed significant improvements, with a MAPE of 2.71 and an RMSE of 0.3124. However, the most substantial enhancement in predictive accuracy was observed with our proposed Hybrid CNN with Autoencoder LSTM (HCAELSTM) model, which achieved the lowest errors among all the models, with a MAPE of 1.175 and an RMSE of 0.1276. In summary, hybrid ML models, especially HCAELSTM, demonstrated superior forecasting accuracy over statistical models like ARIMA, ML models such as SVM and RF, and even the LSTM model, as shown in table 1.

Another set of comparison results is presented in table 2, highlighting the performance of various traditional methods versus our proposed hybrid model using MAE and MSE evaluation metrics. The results clearly indicate that our hybrid model outperforms other state-of-the-art conventional models. Specifically, our proposed HCAELSTM model achieved the lowest scores with an MAE of 0.0782 and an MSE of 0.0162 for Daily Power Production parameters. In comparison, the LSTM model had an MAE of 0.2994 and an MSE of 0.117, while ARIMA had the highest error rates with an MAE of 0.9389 and an MSE of 0.3669. Similarly, for Peak Grid Power

Table 3. Hybrid model sequential steps for prediction.

Layer (type)	Output shape	Param #
conv1d_1 (Conv1D)	(None, 3, 64)	192
max_pooling1d_1 (MaxPooling1D)	(None, 1, 64)	0
flatten_1 (Flatten)	(None, 64)	0
dense_2 (Dense)	(None, 50)	3250
dense_3 (Dense)	(None, 1)	51
lstm (LSTM)	(None, 4, 10)	480
lstm_1 (LSTM)	(None, 4, 6)	408
lstm_2 (LSTM)	(None, 1)	32
repeat_vector (RepeatVector)	(None, 1, 1)	0
lstm_3 (LSTM)	(None, 1, 10)	480
lstm_4 (LSTM)	(None, 1, 10)	840
dense_4 (Dense)	(None, 1, 1)	11
Total params: 5744		
Trainable params: 5744		
Non-trainable params: 0		
None		
dict_keys (['mse', 'mae', 'val_mse', 'val_mae'])		

Production and Solar Radiance, ARIMA showed the highest MAE and MSE scores. SVM performed better than ARIMA, RF outperformed SVM, and LSTM outperformed RF. However, our proposed HCAELSTM model consistently achieved the lowest MAE and MSE scores, demonstrating superior predictive accuracy across all parameters.

The study involves analyzing real-time data from a solar power plant over one year, focusing on three key parameters Daily Power Production in (kWh), Peak Grid Power Production in (MW), and Solar Radiance in (MJ·m−2). The objective was to develop ML models to forecast future data for these parameters. After reviewing existing research, we chose RNN and LSTM models due to their successful performance in related tasks. While both models achieved satisfactory results, LSTM outperformed RNN. To enhance forecast accuracy, the study implemented the Autoencoder LSTM (AELSTM) model, which showed improved prediction capabilities. Subsequent efforts led to the development of a novel hybrid model combining CNN and Autoencoder LSTM (HCAELSTM), which surpassed the other models. The AELSTM model provided better results than simple LSTM, with greater prediction accuracy and reduced error rates. Nevertheless, the hybrid HCAELSTM model excelled beyond all other models, achieving the highest precision and lowest errors in forecasts. The study details its findings through visualizations and tables, highlighting the hybrid model's notable improvements and its potential for accurate solar power generation forecasting.

The hybrid model's parameters and structure are described in table 3, revealing a total of 5,744 trainable parameters available for training. The model does not contain any non-trainable variables, emphasizing its full adaptability during training. The table includes dictionary keys such as 'mae', 'mse', 'val_mse', and 'val_mae' that correspond to various loss metrics used to assess the model's performance. These metrics, including Mean Squared Error (MSE) and Mean Absolute Error (MAE), provide insight into how well the model is functioning. Overall, table 2 offers essential information about the model's architecture, including layer details, parameter count, and the range of loss metrics used for evaluating its performance.

In the experimental phase of this study, specific hardware and software setups were employed. The testing system consisted of an Intel Core i7 processor running at 2.30 GHz with 16 GB of RAM and an NVIDIA RTX 2060 graphics card with 6 GB of GPU memory. The research used TensorFlow version 2.16.1 and Keras version 2.16 libraries for software development to create DL models. Python 3.12 was the programming language of choice for this research. The model was optimized using the Adam optimizer with a learning rate of 0.01, running for 100 epochs with a batch size of 32.

We are taking one year of real-time data of three crucial parameters and then forecasting these parameters for the next year. In our dataset, there are outliers that we removed through a rigorous data cleaning process involving statistical methods such as the Z-score method and IQR (Interquartile Range) to detect and eliminate extreme values that could skew the analysis. Additionally, the dataset exhibits significant variations due to different weather conditions, as this data is from Pakistan, where weather variation is notable throughout the year. In the different weather conditions, as seen in figure 8, it is evident there are more than 50 days in different months of the year when daily power production is less than 400,000 KWh, which is entirely due to variations in weather conditions. Testing the stability of our model by introducing outliers or simulating different weather conditions further validates its robustness. Our hybrid model, HCAELSTM, which combines CNN and

Table 4. MAE and MSE comparison table between RNN, LSTM, AELSTM and Hybrid HCAELSTM.

Models	Daily power production		Peak grid power production		Solar radiance	
	MAE (KWh)	MSE	MAE (MW)	MSE	MAE (MJ/m^2)	MSE
RNN	0.37666	0.13650	0.23327	0.03915	0.26714	0.11567
LSTM	0.22233	0.09761	0.12196	0.03869	0.16188	0.05427
AELSTM	0.11735	0.02444	0.06094	0.0096	0.11257	0.02482
HCAELSTM	0.07823	0.01629	0.04062	0.00646	0.07504	0.01654

Autoencoder LSTM, performs exceptionally well under these varying conditions, making it more comprehensive and reliable for real-world applications. This capability to handle outliers and adapt to diverse weather patterns underscores the superiority of our model over traditional and standalone models.

Real-time data that was gathered over the course of a year makes up the dataset. 80 percent of the dataset is put aside for the RNN model, the LSTM model, the AELSTM model, and the hybrid HCAELSTM model training. The remaining 20 percent is set aside for validation and testing. Every model's losses are assessed and shown using graphical representations.

The HCAELSTM model demonstrates strong performance across multiple parameters in the given table 4. For Daily Power Production, it achieves a Mean Absolute Error (MAE) of 0.07823 KWh and a Mean Squared Error (MSE) of 0.01629. In forecasting Peak Grid Power Production, the model attains an MAE of 0.04062 MW and an MSE of 0.00646. For Solar Radiance, it records an MAE of 0.07504 MJ m^{-2} and an MSE of 0.01654. These results highlight the model's accuracy and robustness in predicting key metrics related to power production and solar radiance.

Figure 10(a) shows comparison of Mean Absolute Error (MAE) between the RNN, LSTM, AELSTM, and hybrid HCAELSTM models for the Daily Power Production parameter shows a clear progression in accuracy over 100 epochs. At the beginning (epoch 0), the RNN model had the highest MAE of 3.2766, while the LSTM, AELSTM, and HCAELSTM models had significantly lower MAEs of 0.5294, 0.9131, and 0.4786, respectively. As training progressed, all models improved, but the hybrid HCAELSTM consistently outperformed the others. By epoch 99, the MAE values were 0.3767 for the RNN, 0.2223 for the LSTM, 0.1402 for the AELSTM, and 0.0782 for the HCAELSTM. This data illustrates the superior predictive capability of the HCAELSTM model, demonstrating its effectiveness in minimizing prediction errors for daily power production over time.

Similarly, figure 10(b) shows the comparison of validation Mean Absolute Error (MAE) between the RNN, LSTM, AELSTM, and hybrid HCAELSTM models for the Daily Power Production parameter indicates significant differences in performance over 100 epochs. At the initial epoch (epoch 0), the RNN model had the highest MAE of 5.2432, followed by the AELSTM at 0.5009, LSTM at 0.4625, and HCAELSTM at 0.4312. This initial evaluation shows that the hybrid HCAELSTM model began with a lower MAE compared to the other models. As the training progressed, all models showed improvement, with the hybrid HCAELSTM model consistently outperforming the others. By epoch 99, the RNN model's MAE had decreased to 0.3796, while the LSTM and AELSTM models achieved lower MAEs of 0.2243 and 0.1216, respectively. The HCAELSTM model maintained the lowest MAE of 0.0755 at the final epoch, demonstrating its superior ability to minimize prediction errors in the daily power production parameter. This trend highlights the effectiveness of the hybrid HCAELSTM model in achieving higher accuracy and reliability compared to the RNN, LSTM, and AELSTM models.

The validation MAE comparison between the RNN, LSTM, AELSTM, and hybrid HCAELSTM models for the Peak Grid Power Production parameter reveals distinct performance differences over 100 epochs shown in figure 10(c). At the initial epoch (epoch 0), the RNN model had the highest MAE of 3.0758, while the LSTM, AELSTM, and HCAELSTM models started with lower MAEs of 0.4418, 1.3395, and 0.4636, respectively. By the final epoch (epoch 99), the RNN model's MAE had decreased to 0.2333, showing significant improvement. The LSTM model achieved an MAE of 0.1220, the AELSTM model reached 0.1032, and the hybrid HCAELSTM model consistently maintained the lowest MAE of 0.0406. This trend demonstrates that the HCAELSTM model outperformed the other models, providing the most accurate predictions for the Peak Grid Power Production parameter across all epochs.

In comparing the validation MAE between the RNN, LSTM, AELSTM, and hybrid HCAELSTM models for the Peak Grid Power Production parameter, notable differences are observed in figure 10(d). At the first epoch, the RNN model starts with the highest MAE at 2.6211, whereas the LSTM, AELSTM, and HCAELSTM models exhibit lower initial MAEs of 0.3946, 0.5059, and 0.4313, respectively. By the final epoch (epoch 99), the RNN model's MAE decreases to 0.2196, indicating substantial improvement. The LSTM model achieves an MAE of 0.1219, the AELSTM model reaches 0.0855, and the hybrid HCAELSTM model consistently maintains the

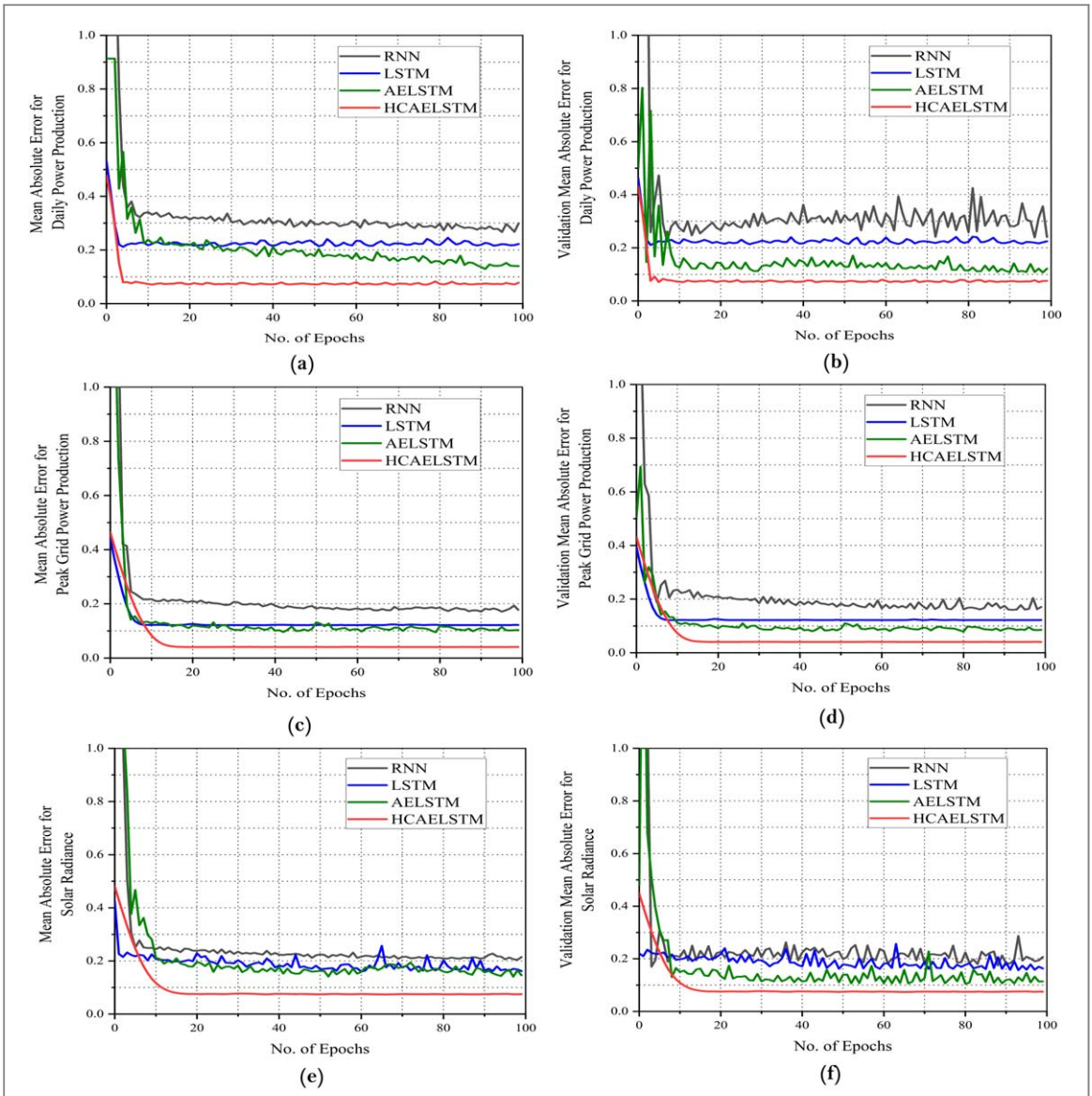

Figure 10. MAE through RNN, LSTM, AELSTM, HCAELSTM models. (a) Actual MAE of daily power production; (b) Validation MAE of daily power production; (c) Actual MAE of peak grid power production; (d) Validation MAE of peak grid power production; (e) Actual MAE of solar radiance; (f) Validation MAE of solar radiance.

lowest MAE at 0.0405. These results demonstrate that the hybrid HCAELSTM model outperforms the other models, offering the most accurate predictions for the Peak Grid Power Production parameter across the epochs.

Figure 10(e) present the comparing the MAE between the RNN, LSTM, AELSTM, and hybrid HCAELSTM models for the Solar Radiance parameter, significant differences are evident. At the first epoch, the RNN model starts with the highest MAE at 2.4041, while the LSTM, AELSTM, and HCAELSTM models exhibit lower initial MAEs of 0.4250, 1.3862, and 0.4813, respectively. By the final epoch (epoch 99), the RNN model's MAE decreases to 0.2671, indicating a substantial improvement. The LSTM model achieves an MAE of 0.1619, the AELSTM model reaches 0.1461, and the hybrid HCAELSTM model consistently maintains the lowest MAE at 0.0750. These results demonstrate that the hybrid HCAELSTM model outperforms the other models, providing the most accurate predictions for the Solar Radiance parameter across the epochs.

Similarly, figure 10(f) present the comparing the validation MAE for the Solar Radiance parameter across RNN, LSTM, AELSTM, and hybrid HCAELSTM models, notable differences emerge from the first to the last epoch. At the first epoch, the RNN model starts with a high MAE of 3.6558, whereas the LSTM, AELSTM, and HCAELSTM models show significantly lower initial MAEs of 0.2201, 0.4805, and 0.4488, respectively. By the final epoch (epoch 99), the RNN model's MAE decreases to 0.2509, showing substantial improvement. The LSTM model achieves an MAE of 0.1633, while the AELSTM model reaches 0.1137. The hybrid HCAELSTM model consistently maintains the lowest MAE, ending at 0.0749. These results highlight the superior

Table 5. R and R^2 Comparison table between RNN, LSTM, AELSTM and Hybrid HCAELSTM.

Parameter	RNN		LSTM		AELSTM		HCAELSTM	
	R	R^2	R	R^2	R	R^2	R	R^2
Daily Power Production	0.674	0.453	0.782	0.610	0.910	0.826	0.961	0.922
Peak Grid Power Production	0.659	0.434	0.778	0.604	0.897	0.805	0.949	0.901
Solar Radiance	0.681	0.461	0.771	0.594	0.901	0.811	0.956	0.912

Table 6. MAPE and RMSE comparison table between RNN, LSTM, AELSTM and Hybrid HCAELSTM.

Parameter	RNN		LSTM		AELSTM		HCAELSTM	
	MAPE	RMSE	MAPE	RMSE	MAPE	RMSE	MAPE	RMSE
Daily Power Production	3.512	0.3692	2.713	0.3124	1.221	0.1564	1.175	0.1276
Peak Grid Power Production	2.771	0.1985	2.434	0.1967	2.282	0.0979	2.116	0.0803
Solar Radiance	4.680	0.3401	3.362	0.2328	2.131	0.1576	1.592	0.1286

performance of the hybrid HCAELSTM model in providing the most accurate predictions for the Solar Radiance parameter.

Table 5 presents the correlation coefficient (R) and the coefficient of determination (R^2) for the HCAELSTM model across different parameters. For Daily Power Production, the model achieves an R value of 0.961 and an R^2 value of 0.922. In forecasting Peak Grid Power Production, it attains an R value of 0.949 and an R^2 value of 0.901. For Solar Radiance, the model records an R value of 0.956 and an R^2 value of 0.912. These high values indicate the model's strong predictive accuracy and reliability.

A lower MAE score signifies that the model's predictions are more precise, closely matched actual values. The mathematical representation of the MAE is articulated in equation (15).

$$\mathrm{MAE} = \frac{1}{N}\sum_{n=1}^{N}|\overline{x_n} - x_n| \tag{19}$$

[Where $\overline{x_n}$ reflects the predicted value, x_n reflects the real value and N is total quantity of data.

Table 6 shows the MAPE and RMSE comparison among our models. The results reveal that our proposed HCAELSTM model has lower MAPE and RMSE values compared to other models across each parameter.

Figure 11(a) comparing the MSE for the Daily Power Production parameter across RNN, LSTM, AELSTM, and hybrid HCAELSTM models, distinct trends are observed. At the initial epoch, the RNN model exhibits a high MSE of 5.2130, while the LSTM, AELSTM, and HCAELSTM models show significantly lower values of 0.3269, 0.9771, and 0.3604, respectively. By the final epoch (epoch 99), the RNN model reduces its MSE to 0.1381. In contrast, the LSTM model achieves a lower MSE of 0.0975, the AELSTM model records 0.0356, and the HCAELSTM model consistently outperforms the others with the lowest MSE of 0.0166. This indicates the superior accuracy and effectiveness of the hybrid HCAELSTM model for predicting Daily Power Production.

Figure 11(b) illustrate the comparing of validation MSE for the Daily Power Production parameter across RNN, LSTM, AELSTM, and hybrid HCAELSTM models, notable differences emerge. At the initial epoch, the RNN model shows a high MSE of 10.1156, while the LSTM, AELSTM, and HCAELSTM models have significantly lower values of 0.2576, 0.3163, and 0.2940, respectively. By the final epoch (epoch 99), the RNN model reduces its MSE to 0.1365. The LSTM model achieves a slightly lower MSE of 0.0976, the AELSTM model records 0.0334, and the HCAELSTM model consistently outperforms the others with the lowest MSE of 0.0163. This demonstrates the superior validation accuracy of the hybrid HCAELSTM model for predicting Daily Power Production.

In the comparison of MSE for Peak Grid Power Production as shown in figure 11(c), the RNN model starts with a high MSE of 3.6249, while the LSTM, AELSTM, and HCAELSTM models show significantly lower initial MSE values of 0.2163, 2.4311, and 0.3291, respectively. As the training progresses, the RNN model reduces its MSE to 0.0490 by the final epoch (epoch 99). The LSTM model achieves a much lower final MSE of 0.0387, and the AELSTM model improves to 0.0250. Notably, the HCAELSTM model consistently outperforms all other models, achieving the lowest final MSE of 0.0065. This indicates the superior accuracy and effectiveness of the HCAELSTM model for predicting Peak Grid Power Production.

Figure 11(d) present the comparison of validation MSE for Peak Grid Power Production, the RNN model begins with a high MSE of 3.3409, while the LSTM, AELSTM, and HCAELSTM models show significantly lower initial MSE values of 0.1773, 0.2815, and 0.2848, respectively. As the training progresses, the RNN model

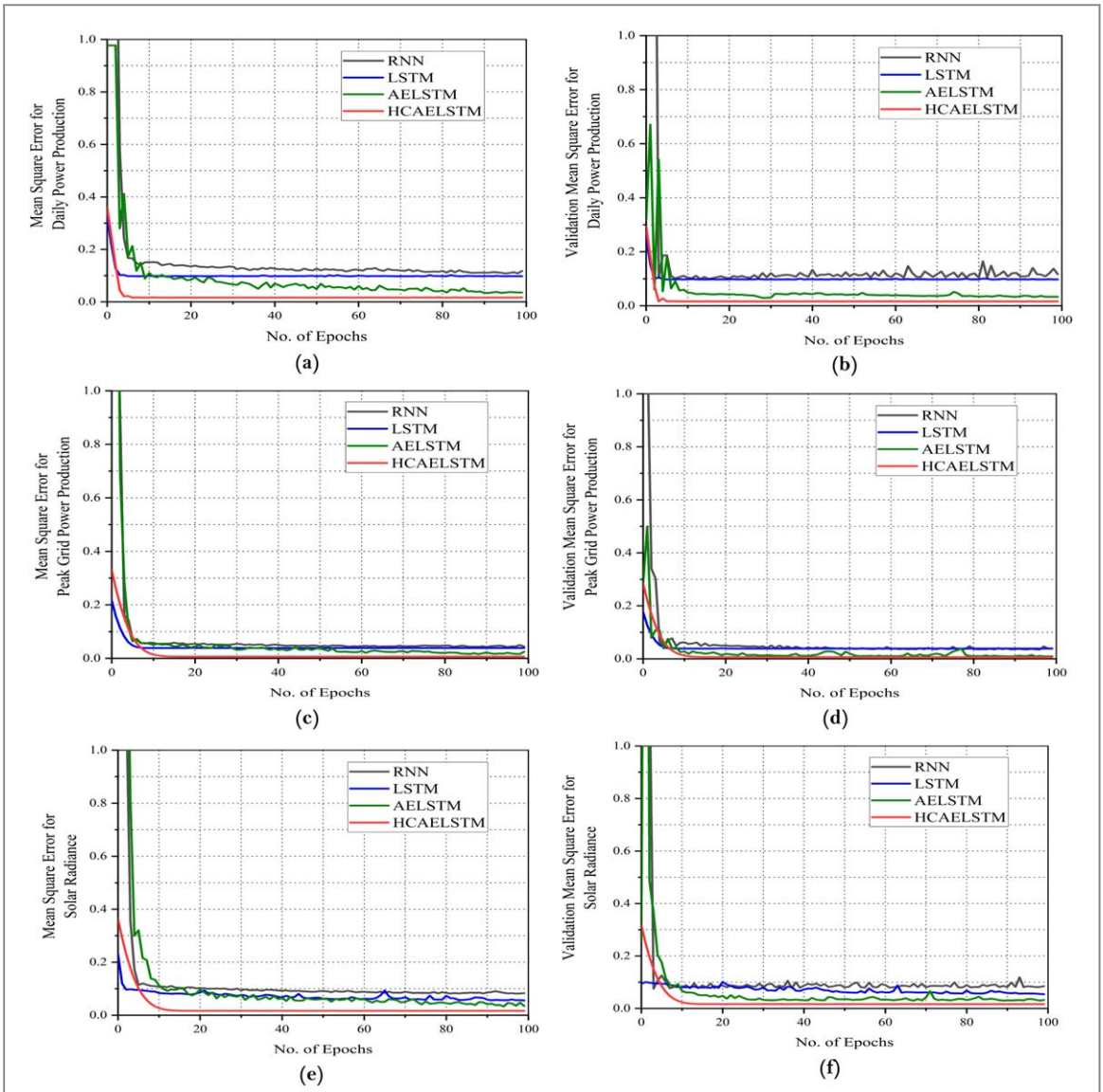

Figure 11. MSE through RNN, LSTM, AELSTM, HCAELSTM. (a) Actual MSE of daily power production; (b) Validation MSE of daily power production; (c) Actual MSE of peak grid power production; (d) Validation MSE of peak grid power production; (e) Actual MSE of solar radiance; (f) Validation MSE of solar radiance.

reduces its MSE to 0.0392 by the final epoch (epoch 99). The LSTM model achieves a final MSE of 0.0387, and the AELSTM model improves to 0.0093. Notably, the HCAELSTM model consistently outperforms all other models, achieving the lowest final MSE of 0.0065. This indicates the superior accuracy and effectiveness of the HCAELSTM model for predicting Peak Grid Power Production in the validation set.

Figure 11(e) illustrate the comparison of validation MSE for the Solar Radiance parameter, the RNN model starts with a high MSE of 4.0598, while the LSTM, AELSTM, and HCAELSTM models have lower initial MSE values of 0.2311, 2.8499, and 0.3639, respectively. Over the epochs, the RNN model reduces its MSE to 0.1104 by epoch 99. The LSTM model performs better, achieving a final MSE of 0.0557. The AELSTM model shows significant improvement, bringing its MSE down to 0.0349. However, the HCAELSTM model consistently outperforms the others, achieving the lowest final MSE of 0.0166, indicating its superior accuracy in predicting Solar Radiance.

In the comparison of validation MSE for the Solar Radiance parameter as shown in figure 11(f), the RNN model starts with a high MSE of 7.2767, whereas the LSTM, AELSTM, and HCAELSTM models have significantly lower initial MSE values of 0.0937, 0.2575, and 0.3177, respectively. Over the epochs, the RNN model reduces its MSE to 0.1157 by epoch 99. The LSTM model performs better, achieving a final MSE of 0.0543. The AELSTM model shows further improvement, bringing its MSE down to 0.0321. However, the HCAELSTM model consistently outperforms the others, achieving the lowest final MSE of 0.0165, indicating its superior accuracy in predicting Solar Radiance.

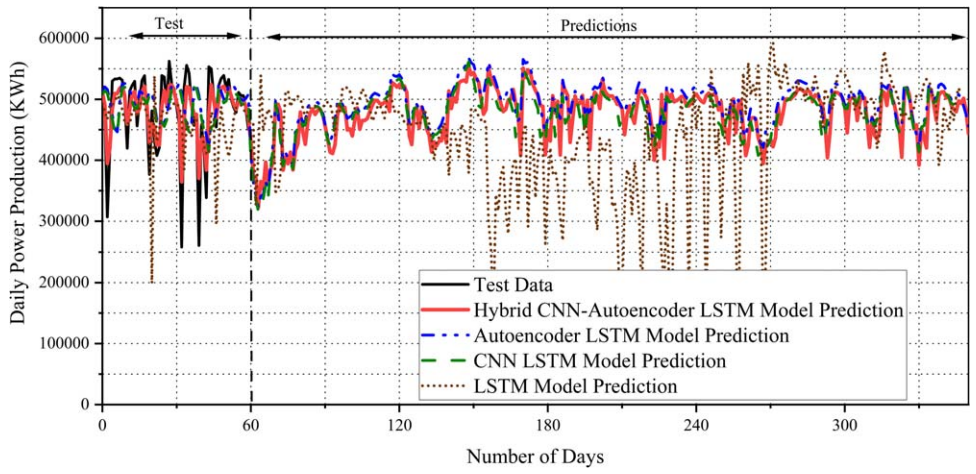

Figure 12. Comparison of tested and forecasted data for daily power production in a solar plant.

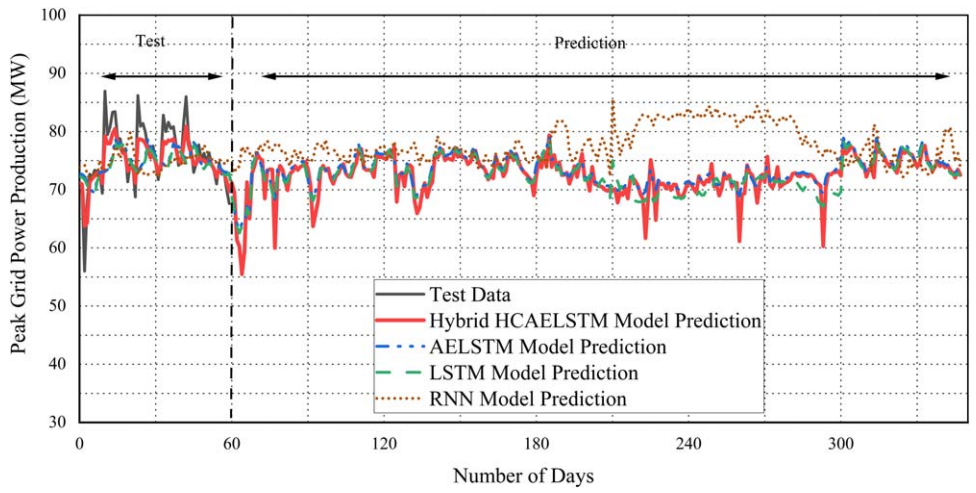

Figure 13. Comparison of tested and forecasted data for peak grid power production in a solar plant.

A lower MSE value indicates that the forecasts made by the model were more accurate and closely matched actual values. The mathematical formulation of the MSE is depicted by equation (16).

$$\mathrm{MSE} = \frac{1}{N}\sum_{n=1}^{N}(\overline{x_n} - x_n)^2 \tag{20}$$

Where $\overline{x_n}$ reflects the predicted value, x_n reflects the real value and N is total quantity of data.

Although our proposed hybrid CNN-Autoencoder LSTM (HCAELSTM) model has shown impressive predictive accuracy for solar power parameters, its practical application depends on several factors. The potential implementation of the HCAELSTM model is closely tied to industry readiness, resource availability, and the effectiveness of knowledge transfer. A thorough evaluation of these factors will provide valuable insights into the model's feasibility for integration within solar plant operations. The likelihood of implementing the HCAELSTM model in real-time grid management software is highly favorable due to its proven ability to forecast crucial parameters for efficient grid operations. With its adaptability to real-time data, customization options, and continuous feedback capabilities, the model is well-suited to the evolving demands of dynamic grid management. This alignment promises increased forecasting accuracy over time and significant support for cost efficiency and renewable energy integration, making the HCAELSTM model a practical choice for real-time grid management software development.

A detailed examination of the predicted results from a 100 MW solar power plant is presented in figures 12–14. The research evaluates forecasts from four ML models trained on three major parameters: Daily Power Production (kWh), Peak Grid Power Generation (MW), and Solar Radiance (MJ/m^2). The models are

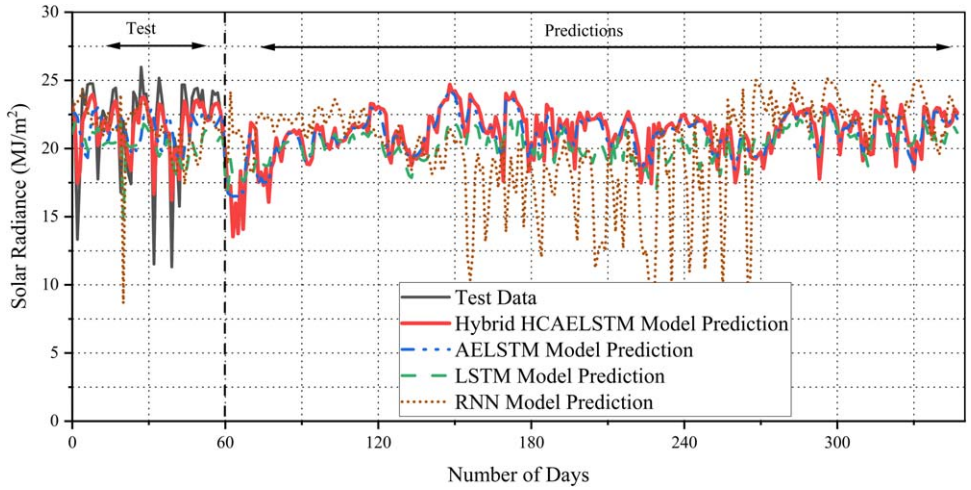

Figure 14. Comparison of tested and forecasted data for solar radiance in a solar plant.

RNN, LSTM, AELSTM, and a hybrid HCAELSTM. The yearly real-time data, 80% was utilized for training the models, while testing and validation were done with the leftover 20%. The 60-day plant's test data is compared with the actual forecasts in the first set of graphics, then forecasts the three parameters for the upcoming year. The models' performance also accuracy can be evaluated by comparing the graphs representing the test and prediction data.

Figure 12 presents a comparative analysis of daily power production predictions over approximately 365 days using four models: our proposed Hybrid HCAELSTM, AELSTM, LSTM, and RNN, against the actual test data with the y-axis spanning from 1×10^5 kWh to 7×10^5 kWh, and the x-axis depicting days in sequence. The test phase encompasses the initial 60 days, while the subsequent period is used for prediction evaluation. The Hybrid HCAELSTM model (red) demonstrates a superior ability to mirror the test data closely throughout the entire period. Its predictions exhibit minimal deviation from the actual data, indicating a strong capability to capture both the short-term fluctuations and long-term trends in daily power production. This suggests that the hybrid model effectively leverages the strengths of its combined components CNN, Autoencoder and LSTM yielding highly accurate forecasts. The AELSTM model (blue) and the LSTM model (green) also perform well, maintaining a relatively close alignment with the actual data. However, their predictions show slightly greater variability compared to the Hybrid HCAELSTM model. This suggests that while these models can capture the general pattern of daily power production, they are somewhat less adept at handling the intricate fluctuations present in the data. The AELSTM model, incorporating autoencoders, performs slightly better than the standard LSTM, reflecting the benefit of additional feature extraction. The RNN model (brown), on the other hand, shows the least accurate predictions among the models. Its predictions exhibit significant variability and frequently diverge from the actual test data, particularly in the latter part of the timeline (beyond 150 days). This suggests that the RNN model struggles to effectively capture the complex temporal dependencies and patterns inherent in the daily power production data, leading to less reliable forecasts. In particular, table 6 highlights that the hybrid model achieves a lower MAPE error score of 1.175, whereas the other models AELSTM (1.221), LSTM (2.713), and RNN (3.512) have higher MAPE scores. In summary, the Hybrid HCAELSTM model outperforms the other models in terms of accuracy and consistency in predicting daily power production. Its ability to closely track the actual data highlights the efficacy of combining CNN, autoencoder and LSTM architectures for time-series forecasting tasks. The AELSTM and LSTM models also provide competent predictions but fall short in handling finer details compared to the hybrid approach. The RNN model, while capable of following the general trend, fails to offer precise and stable predictions, underscoring the advantages of more sophisticated architectures like the proposed Hybrid HCAELSTM model for such complex forecasting tasks.

Figure 13 illustrates the performance of four different models, our proposed Hybrid HCAELSTM, AELSTM, LSTM, and RNN in predicting the Peak Grid Power Production with the vertical axis spanning from 30 MW to 100 MW and the horizontal axis depicting a period of approximately 365 days. The test data is depicted in black, with the predictions of the Hybrid HCAELSTM model shown in red, the AELSTM model in blue, the LSTM model in green, and the RNN model in brown. From the figure, it is evident that all models generally follow the trend of the actual test data. However, there are notable differences in the accuracy and consistency of the predictions among the models. The Hybrid HCAELSTM model's predictions (red) closely track the actual test

data, especially after the initial test phase (first 60 days). This suggests that the hybrid model effectively captures the underlying patterns in the data, likely benefiting from the combined strengths of both convolutional and LSTM components. In contrast, the AELSTM model (blue) and LSTM model (green) show similar patterns, though with slightly more variability compared to the Hybrid HCAELSTM model. They tend to miss some of the more extreme peaks and troughs, indicating potential limitations in capturing short-term fluctuations in the data. Nonetheless, these models perform reasonably well overall, maintaining a consistent approximation of the actual values. The RNN model (brown), however, demonstrates the least accurate predictions, particularly noticeable in the latter part of the timeline (beyond 180 days). The RNN model's predictions exhibit higher variance and fail to align closely with the actual test data, suggesting that it struggles more with capturing the temporal dependencies and complex patterns inherent in the time series data compared to the other models. Additionally, table 6 provides insight into the models' performance differences, showcasing their MAPE scores. The hybrid HCAELSTM model achieves an impressively low MAPE score of 2.116, indicating its predictions are very accurate and closely align with the actual data. In comparison, AELSTM has a MAPE of 2.282, LSTM scores 2.434, and RNN has the highest MAPE of 2.771. In summary, the Hybrid HCAELSTM model outperforms the other models in terms of accuracy and consistency, effectively capturing both short-term fluctuations and long-term trends in the peak grid power production data. The AELSTM and LSTM models, while competent, exhibit slight deficiencies in tracking rapid changes. The RNN model, on the other hand, shows significant limitations in its predictive capability, highlighting the advantage of using more sophisticated architectures like hybrid models for time-series forecasting tasks.

Figure 14 presents a comparison of Solar Radiance predictions over a period of approximately 365 days using four models: Hybrid HCAELSTM, AELSTM, LSTM, and RNN, against the actual test data with the vertical axis spanning from 0 to 30 MJ m^{-2} and the horizontal axis representing the total days in number. The Hybrid HCAELSTM model is the proposed model in this analysis, shown in red, while the test data is depicted in black. The test phase covers the initial 60 days, followed by the prediction phase for the remainder of the period. The Hybrid HCAELSTM model demonstrates a strong ability to track the actual solar radiance data closely throughout the entire period. Its predictions exhibit minimal deviation from the test data, indicating a high degree of accuracy and consistency. This model leverages the strengths of convolutional neural networks (CNN) for feature extraction, autoencoders for dimensionality reduction and noise removal, and long short-term memory (LSTM) networks for capturing temporal dependencies, resulting in superior predictive performance. The combination of these components enables the Hybrid HCAELSTM model to effectively manage the complex patterns and variability inherent in solar radiance data. The AELSTM model (blue) and the LSTM model (green) also perform reasonably well, maintaining a relatively close alignment with the actual data. However, their predictions show slightly greater variability compared to the Hybrid HCAELSTM model. This suggests that while these models can capture the general pattern of solar radiance, they are somewhat less adept at handling the intricate fluctuations and noise present in the data. The AELSTM model, which incorporates autoencoders, performs slightly better than the standard LSTM, reflecting the benefit of additional feature extraction and noise reduction. The RNN model (brown), however, shows the least accurate predictions among the models. Its predictions exhibit significant variability and frequently diverge from the actual test data, particularly in the latter part of the timeline (beyond 160 days). This suggests that the RNN model struggles to effectively capture the complex temporal dependencies and patterns inherent in the solar radiance data, leading to less reliable forecasts. Table 6 presents the performance variations among the different models, showcasing their MAPE scores. The hybrid HCAELSTM model achieves an impressively low MAPE score of 1.592, indicating its predictions are highly accurate and closely match the actual data. By contrast, AELSTM records a MAPE of 2.131, LSTM scores 3.362, and RNN shows the highest MAPE of 4.680. In summary, the Hybrid HCAELSTM model outperforms the other models in terms of accuracy and consistency in predicting solar radiance. Its ability to closely track the actual data highlights the efficacy of combining CNN's feature extraction capabilities with the autoencoder and LSTM architectures for time-series forecasting tasks. The AELSTM and LSTM models also provide competent predictions but fall short in handling finer details compared to the hybrid approach. The RNN model, while capable of following the general trend, fails to offer precise and stable predictions, underscoring the advantages of more sophisticated architectures like the proposed Hybrid HCAELSTM model for such complex forecasting tasks.

6. Conclusion

The study's results demonstrate the clear superiority of the Hybrid HCAELSTM model across all accuracy and performance metrics. It consistently outperformed the AELSTM, LSTM, and RNN models. For instance, the HCAELSTM model achieved an RMSE of 0.1276 for 'Daily Power Production,' surpassing AELSTM's RMSE of 0.1562, and recorded an RMSE of 0.0803 for 'Peak Grid Power Production,' significantly better than AELSTM's

0.0979, and an RMSE of 0.1286 for 'Solar Radiance,' outperforming AELSTM's 0.1576. These findings have substantial implications for smart grid operations, particularly in enhancing the accuracy of forecasting Daily Power Production, Peak Grid Power Production, and Solar Radiance. The HCAELSTM model's improved accuracy enables a better balance of supply and demand, optimizes the integration of renewable energy sources, reduces the likelihood of power outages, and enhances grid reliability and efficiency. The study underscores the critical role of AI and ML in advancing smart grid technology. Accurate forecasting of solar radiance and peak grid power production is essential for optimizing energy production and ensuring grid stability. The superior performance of the HCAELSTM model supports more efficient and sustainable energy management, driving the transition to a resilient energy future.

Future research should explore alternative algorithms for power prediction, new hybrid models, and additional factors like grid load data to enhance forecast accuracy. Applying these models to other renewable energy sources, improving real-time forecasting systems, and investigating resilience to unexpected events will further advance smart grid management, leading to a more intelligent and sustainable energy future.

Acknowledgments

This work was supported by Princess Nourah bint Abdulrahman University Researchers Supporting Project number (PNURSP2024R51), Princess Nourah bint Abdulrahman University, Riyadh, Saudi Arabia

Data availability statement

The data that support the findings of this study are openly available at the following URL/DOI: https://github.com/DashanTJU/Solar-Forecasting.

Data and model code availability

Data and model code can be found on GitHub at https://github.com/DashanTJU/Solar-Forecasting.

Conflicts of interest

No conflicts of interest to declare.

ORCID iDs

Ahsan Zafar https://orcid.org/0000-0002-2981-9779
Moeed Sehnan https://orcid.org/0009-0008-2316-0855
Usama Afzal https://orcid.org/0000-0002-4039-0627

References

[1] Wang F, Xuan Z, Zhen Z, Li K, Wang T and Shi M 2020 A day-ahead PV power forecasting method based on LSTM-RNN model and time correlation modification under partial daily pattern prediction framework *Energy Convers. Manage.* **212** 112766
[2] Khanlari A, Sözen A, Şirin C, Tuncer A D and Gungor A 2020 Performance enhancement of a greenhouse dryer: analysis of a cost-effective alternative solar air heater *J. Clean. Prod.* **251** 119672
[3] Mishra S, Gaikwad S B and Singh T 2024 Machine learning guided strategies to develop high efficiency indoor perovskite solar cells *Advanced Theory and Simulations* **7** 2301193
[4] Gersnoviez A, Gámez-Granados J C, Cabrera-Fernández M, Santiago I, Cañete-Carmona E and Brox M 2023 Neuro-fuzzy systems for daily solar irradiance classification and PV efficiency forecasting *Alexandria Engineering Journal* **79** 21–33
[5] Wu X, Yang C, Han W and Pan Z 2022 Integrated design of solar photovoltaic power generation technology and building construction based on the Internet of Things *Alexandria Engineering Journal* **61** 2775–86
[6] Lima M A F, Carvalho P C, Fernández-Ramírez L M and Braga A P 2020 Improving solar forecasting using deep learning and portfolio theory integration *Energy* **195** 117016
[7] Li K, Wang F, Mi Z, Fotuhi-Firuzabad M, Duić N and Wang T 2019 Capacity and output power estimation approach of individual behind-the-meter distributed photovoltaic system for demand response baseline estimation *Appl. Energy* **253** 113595
[8] Shah N and Zafar A 2022 Improved performance of silicon-germanium solar cell based on optimization of layer thickness *City University International Journal of Computational Analysis* **5** 1–10
[9] Ahmed R, Sreeram V, Mishra Y and Arif M D 2020 A review and evaluation of the state-of-the-art in PV solar power forecasting: techniques and optimization *Renew. Sustain. Energy Rev.* **124** 109792
[10] Wang J and Azam W 2024 Natural resource scarcity, fossil fuel energy consumption, and total greenhouse gas emissions in top emitting countries *Geoscience Frontiers* **15** 101757

[11] Frederiksen C A F and Cai Z 2022 Novel ML approach for solar photovoltaic energy output forecast using extra-terrestrial solar irradiance *Appl. Energy* **306** 118152
[12] Jiang Y, Zheng L and Ding X 2021 Ultra-short-term prediction of photovoltaic output based on an LSTM-ARMA combined model driven by EEMD *J. Renew. Sustain. Energy* **13** 046103
[13] Das S 2021 Short term forecasting of solar radiation and power output of 89.6 kWp solar PV power plant *Mater. Today Proc.* **39** 1959–69
[14] Al-Nimr M D A, Kiwan S and Sharadga H 2018 Simulation of a novel hybrid solar photovoltaic/wind system to maintain the cell surface temperature and to generate electricity *Int. J. Energy Res.* **42** 985–98
[15] Jung Y, Jung J, Kim B and Han S 2020 Long short-term memory recurrent neural network for modeling temporal patterns in long-term power forecasting for solar PV facilities: case study of South Korea *J. Clean. Prod.* **250** 119476
[16] Konstantinou M, Peratikou S and Charalambides A G 2021 Solar photovoltaic forecasting of power output using lstm networks *Atmosphere* **12** 124
[17] Lee S and Kim J 2021 SPV dominant parameter estimation exploration and visualization from weather and prediction model *The Transactions of the Korean Institute of Electrical Engineers* **70** 464–5
[18] Su D, Batzelis E and Pal B 2019 ML algorithms in forecasting of photovoltaic power generation *2019 Int. Conf. on Smart Energy Systems and Technologies (SEST)* (IEEE) pp 1–6
[19] Shafiee S and Topal E 2009 When will fossil fuel reserves be diminished? *Energy Policy* **37** 181–9
[20] Koster D, Fiorelli D, Bruneau P and Braun C 2023 Single-site forecasts for 130 photovoltaic systems at distribution system operator level, using a hybrid-physical approach, to improve grid-integration and enable future smart-grid operation *Sol. RRL* **7** 2200652
[21] Sedai A, Dhakal R, Gautam S, Dhamala A, Bilbao A, Wang Q, Wigington A and Pol S 2023 Performance analysis of statistical, machine learning and deep learning models in long-term forecasting of solar power production *Forecasting* **5** 256–84
[22] Nutakki M and Mandava S 2023 Review on optimization techniques and role of Artificial Intelligence in home energy management systems *Eng. Appl. Artif. Intell.* **119** 105721
[23] Ahmad W, Ayub N, Ali T, Irfan M, Awais M, Shiraz M and Glowacz A 2020 Towards short term electricity load forecasting using improved support vector machine and extreme learning machine *Energies* **13** 2907
[24] Yang L and Yang H 2019 Analysis of different neural networks and a new architecture for short-term load forecasting *Energies* **12** 1433
[25] Xu L, Li C, Xie X and Zhang G 2018 Long-short-term memory network based hybrid model for short-term electrical load forecasting *Information* **9** 165
[26] Rodríguez F, Galarza A, Vasquez J C and Guerrero J M 2022 Using deep learning and meteorological parameters to forecast the photovoltaic generators intra-hour output power interval for smart grid control *Energy* **239** 122116
[27] Habbak H, Mahmoud M, Metwally K, Fouda M M and Ibrahem M I 2023 Load forecasting techniques and their applications in smart grids *Energies* **16** 1480
[28] Souhe F G Y, Mbey cf, Boum A T, Ele P and Kakeu V J F 2022 A hybrid model for forecasting the consumption of electrical energy in a smart grid *The Journal of Engineering* **2022** 629–43
[29] Ciechulski T and Osowski S 2021 High precision LSTM model for short-time load forecasting in power systems *Energies* **14** 2983
[30] Pramono S H, Rohmatillah M, Maulana E, Hasanah R N and Hario F 2019 Deep learning-based short-term load forecasting for supporting demand response program in hybrid energy system *Energies* **12** 3359
[31] Alhussein M, Aurangzeb K and Haider S I 2020 Hybrid CNN-LSTM model for short-term individual household load forecasting *IEEE Access* **8** 180544–57
[32] Faheem M, Shah S B H, Butt R A, Raza B, Anwar M, Ashraf M W, Ngadi M A and Gungor V C 2018 Smart grid communication and information technologies in the perspective of Industry 4.0: opportunities and challenges *Computer Science Review* **30** 1–30
[33] Shadab A, Ahmad S and Said S 2020 Spatial forecasting of solar radiation using ARIMA model *Remote Sensing Applications: Society and Environment* **20** 100427
[34] Kanchana W and Sirisukprasert S 2020 PV power forecasting with holt-winters method *2020 8th Int. Electrical Engineering Congress (iEECON)* (IEEE) pp 1–4
[35] Perveen G, Rizwan M, Goel N and Anand P 2020 Artificial neural network models for global solar energy and photovoltaic power forecasting over India *Energy Sources Part*A **42** 1–26
[36] Jiang Y, Zheng L and Ding X 2021 Ultra-short-term prediction of photovoltaic output based on an LSTM-ARMA combined model driven by EEMD *J. Renewable Sustainable Energy* **13** 461031–12
[37] Liu L, Zhao Y, Chang D, Xie J, Ma Z, Sun Q, Yin H and Wennersten R 2018 Prediction of short-term PV power output and uncertainty analysis *Appl. Energy* **228** 700–11
[38] Ibañez J A, Benitez I B, Cañete J M, Magadia J C and Principe J A 2023 Accuracy assessment of satellite-based and reanalysis solar irradiance data for solar PV output forecasting using SARIMAX *J. Renewable Sustainable Energy* **15** 066101
[39] Fara L, Diaconu A, Craciunescu D and Fara S 2021 Forecasting of energy production for photovoltaic systems based on ARIMA and ANN advanced models *Int. J. Photoenergy* **2021** 1–19
[40] Srivastava R, Tiwari A N and Giri V K 2019 Solar radiation forecasting using MARS, CART, M5, and random forest model: a case study for India *Heliyon* **5** 02692
[41] Gao M, Li J, Hong F and Long D 2019 Short-term forecasting of power production in a large-scale photovoltaic plant based on LSTM *Applied Sciences* **9** 3192
[42] Zhou Y, Zhou N, Gong L and Jiang M 2020 Prediction of photovoltaic power output based on similar day analysis, genetic algorithm and extreme learning machine *Energy* **204** 117894
[43] Islam S Z, Othman M L, Saufi M, Omar R, Toudeshki A and Islam S Z 2020 Photovoltaic modules evaluation and dry-season energy yield prediction model for NEM in Malaysia *PLoS One* **15** e0241927
[44] Mishra M, Nayak J, Naik B and Abraham A 2020 Deep learning in electrical utility industry: a comprehensive review of a decade of research *Eng. Appl. Artif. Intell.* **96** 104000
[45] Yu Y, Cao J and Zhu J 2019 An LSTM short-term solar irradiance forecasting under complicated weather conditions *IEEE Access* **7** 145651–66
[46] Kim E, Akhtar M S and Yang O B 2023 Designing solar power generation output forecasting methods using time series algorithms *Electr. Power Syst. Res.* **216** 109073
[47] Jamil I, Lucheng H, Iqbal S, Aurangzaib M, Jamil R, Kotb H, Alkuhayli A and AboRas K M 2023 Predictive evaluation of solar energy variables for a large-scale solar power plant based on triple deep learning forecast models *Alexandria Engineering Journal* **76** 51–73
[48] Zheng J, Du J, Wang B, Klemeš J J, Liao Q and Liang Y 2023 A hybrid framework for forecasting power generation of multiple renewable energy sources *Renew. Sustain. Energy Rev.* **172** 113046

[49] Zhang Y, Qin C, Srivastava A K, Jin C and Sharma R K 2020 Data-driven day-ahead PV estimation using autoencoder-LSTM and persistence model *IEEE Trans. Ind. Appl.* **56** 7185–92
[50] Zafar A, Che Y, Faheem M, Abubakar M, Ali S and Bhutta M S 2024 Machine learning autoencoder-based parameters prediction for solar power generation systems in smart grid *IET Smart Grid* **7** 328–50
[51] Li L L, Cheng P, Lin H C and Dong H 2017 Short-term output power forecasting of photovoltaic systems based on the deep belief net *Advances in Mechanical Engineering* **9** 1687814017715983
[52] Abdel-Nasser M and Mahmoud K 2019 Accurate photovoltaic power forecasting models using deep LSTM-RNN *Neural Computing and Applications* **31** 2727–40
[53] Zafar A, Che Y, Ahmed M, Sarfraz M, Ahmad A and Alibakhshikenari M 2023 Enhancing power generation forecasting in smart grids using hybrid autoencoder long short-term memory machine learning model *IEEE Access* **11** 118521–37
[54] Said Y and Alanazi A 2023 AI-based solar energy forecasting for smart grid integration *Neural Computing and Applications* **35** 8625–34
[55] Sabri M and El Hassouni M 2023 Photovoltaic power forecasting with a long short-term memory autoencoder networks *Soft Computing* **27** 10533–53